LARGE, a putative glycosyltransferase, generates spontaneous muscular dystrophy in the *Large*^{myd} mouse model (16). A unique feature of LARGE is that its overexpression produces a hyperglycosylated α-DG that shows increased laminin binding activity, even in cells with genetic defects in the α-DG glycosylation pathway (17).

Mutations in each of these genes (*POMT1*, *POMT2*, *POMGnT1*, *fukutin*, *FKRP*, and *LARGE*) have been identified in congenital and limb-girdle forms of muscular dystrophy (18). A common characteristic of patients who have such mutations is abnormal glycosylation of α-DG; thus, these conditions are collectively referred to as dystroglycanopathies. The clinical spectrum of dystroglycanopathy is broad, ranging from severe congenital onset associated with structural brain malformations to a milder congenital variant with no brain involvement and to limb-girdle muscular dystrophy type 2 variants with childhood or adult onset (18, 19). Eye abnormalities are often associated with more severe dystroglycanopathy, such as Walker-Warburg syndrome and muscle-eye-brain disease (20). The ophthalmologic phenotype of muscular dystrophy is also known for Duchenne/Becker muscular dystrophy, which is caused by dystrophin mutations. Most patients with Duchenne/Becker muscular dystrophy have evidence of abnormal electroretinograms (ERG) (21).

Pikachurin, the most recently identified DG ligand protein, is localized in the synaptic cleft in the photoreceptor ribbon synapse (22). Like other DG ligands, pikachurin contains LG domains in its C-terminal region. Pikachurin-null mutant mice show improper apposition of the bipolar cell dendritic tips to the photoreceptor ribbon synapses, resulting in altered synaptic signal transmission and visual function. Similar retinal electrophysiological abnormalities, such as attenuated or delayed b-wave, have been observed in *Large*^{myd} (23) and POMGnT1-deficient mice (24). These studies imply a functional relationship between pikachurin and DG glycosylation in the retinal ribbon synapse.

In this study, we have biochemically characterized the interaction between pikachurin and α-DG. We have found that both GlcNAc-β1,2-branch and LARGE-dependent modification on *O*-Man are necessary for the pikachurin-DG interaction. Furthermore, in dystroglycanopathy model animals, pikachurin localization in the retinal synaptic outer plexiform layer is severely disrupted. These data demonstrate that post-translational maturation of DG is essential for pikachurin binding and proper localization, providing a possible molecular explanation for the retinal electrophysiological abnormalities observed in dystroglycanopathy patients.

EXPERIMENTAL PROCEDURES

Vector Construction and Protein Expression—Construction of recombinant mouse pikachurin LG domains (PikaLG; residues 391–1017) has been described previously (22). Single or tandem LG domains were constructed using PCR, with a full-length PikaLG expression vector as the template cDNA. Primers used were as follows: LG1(391–627), PikaKpn (CTTGGTACCGAGCTCGGATC) and E627r (TTCTCGAGCCTCCAGGGGCCAGGGTGTG); LG2(542–838), G542f (TTGGTACCGAGCTCGGATCTGGGAAGAAGATTGACATGAG) and P838r (TTCTCGAGCTGGGATCTCGATGGCTTCTA); LG3(799–1017), D766f (TTGGTACCGAGCTCGGATCTGACCGGACCATCCATGTGAAG) and PikaR (GCAACTAGAAGGCACAGTCG); LG1-2(391–883), PikaKpn and P838r; and LG2-3(542–1017), G542f and PikaR. PCR products were digested with KpnI/XhoI and inserted into the KpnI/XhoI sites of the pSecTag2 vector (Invitrogen).

Recombinant mouse α-DG fused to an Fc tag (DGFc) also has been described previously (22). Deletion mutants were constructed using PCR, with the wild-type DGFc vector as the template cDNA. Primers used were as follows: DG-N(1-313), pCAGf (AAGAATTCGCCGCCACCATGAGG) and DGFc313r (AATCTAGATTTGGGGAGAGTGGGCTTCTT); DGΔN(1–28 plus 315–651), pCAGf and DGFc28r (GGCCTGAGCCACAGCCACAGACAGGAGGAG); and DGFc315f (ACACCTACACCTGTTACTGCC) and Fcexon2r (TCCCCCCAGGAGTTCAGGTGC); DGΔC(1–483), pCAGf and DGFc483r (AATCTAGAAGGAATTGTCAGTGTTGGGCG); DG^{half}(1–407), pCAGf and DGFc407r (AATCTAGAACTGGTGGTAGTACGGATTCG). PCR products were digested with EcoRI/XbaI and inserted into the EcoRI/XbaI sites of the wild-type DGFc expression vector.

PikaLG and DGFc constructs were expressed in HEK293 cells (22). For preparation of PikaLG-containing cell lysates, transfected cells were solubilized in lysis buffer (1% Nonidet P-40, 10% glycerol, 50 mM Tris-HCl, pH 7.5, 150 mM NaCl, and a proteinase inhibitor mixture). The samples were centrifuged at 15,000 rpm for 10 min at 4 °C, and the supernatants were used for binding assays.

DGFc proteins were secreted into the cell culture media and recovered with protein A or protein G beads. For the solid-phase binding assays, DGFc proteins were eluted with 0.1 M glycine HCl, pH 2.5, and then neutralized to a final concentration of 0.2 M Tris-HCl, pH 8.0. Protein concentrations of the cell lysates and the DGFc proteins were determined using Lowry's method (Bio-Rad) with BSA as a standard.

Antibodies—Antibodies used for Western blots and immunofluorescence were as follows: mouse monoclonal antibody 8D5 against β-DG (Novacastra); rabbit polyclonal antibody against β-DG (Santa Cruz Biotechnology); mouse monoclonal antibody IIH6 against α-DG (Upstate); goat polyclonal antibody against the α-DG C-terminal domain (AP-074G-C) (25); and rabbit polyclonal antibodies against pikachurin (22).

Animals—C57BL/6 mice were obtained from Japan SLC, Inc., and *Large*^{myd} mice were obtained from The Jackson Laboratory. Generation of *POMGnT1*-deficient mice has been described previously (26). Mice were maintained in accordance with the animal care guidelines of Osaka University and Kobe University.

Pikachurin Binding Assay—For the DGFc pulldown assay, secreted DGFc proteins were recovered from conditioned media using protein A beads (10 μl). DGFc-protein A bead complexes were washed with TBS (50 mM Tris-HCl, pH 7.4, and 150 mM NaCl) and incubated with cell lysates containing PikaLG proteins in the presence of 2 mM $CaCl_2$ overnight at 4 °C. After five washes with washing buffer (0.1% Nonidet P-40, 50 mM Tris-HCl, pH 7.5, 150 mM NaCl, 2 mM $CaCl_2$), bound materials were eluted with SDS-sample buffer. Bound materials

were analyzed by Western blotting using anti-His or anti-Myc tag antibodies and the anti-Fc antibody.

For the solid-phase binding assays, DGFc preparations (2.5 μg) were coated on ELISA microplates (Costar) for 16 h at 4 °C. Plates were washed in TBS and blocked for 2 h with 3% BSA in TBS. PikaLG-containing cell lysates (8 μg) in binding buffer (3% BSA, 1% Nonidet P-40, 2 mM $CaCl_2$ in TBS) were applied and incubated overnight at 4 °C. Wells were washed with TBS containing 1% BSA, 0.1% Nonidet P-40, and 1 mM $CaCl_2$ for three times and incubated for 30 min with 1:1,000 anti-Myc (Santa Cruz Biotechnology) followed by anti-rabbit HRP. Plates were developed with *o*-phenylenediamine dihydrochloride and H_2O_2. Reactions were stopped with 2 N H_2SO_4, and values were obtained using a microplate reader. BSA-coated wells were used to subtract nonspecific binding. For Ca^{2+} concentration dependence, the data were fit to the equation $A = B_{max}x/(K_d + x)$, where K_d is the concentration required to reach half-maximal binding; A is absorbance, and B_{max} is maximal binding. All data were obtained as the means of triplicate measurements. Each experiment was repeated more than three times, and data are represented as the average of at least three independent experiments with standard deviations. Statistical analysis was performed with a two-tailed paired *t* test (GraphPad prism). A p value of <0.05 was considered to be significant.

For binding assays with PikaLG deletion proteins, we confirmed protein expression via Western blot analysis. Cell lysates containing comparable amounts of each LG deletion protein were adjusted by adding mock-transfected cell lysate to achieve a normalized total protein concentration across reaction mixtures.

DG Enrichment and Immunoprecipitation—For solid-phase binding assays with brain DG, mouse brain tissue (200 mg) was homogenized in 1.8 ml of TBS with a proteinase inhibitor mixture and then solubilized with 1% Triton X-100. Samples were centrifuged at 15,000 rpm for 10 min, and the supernatants were incubated with 50 μl of wheat germ agglutinin-agarose beads (Vector Laboratories) overnight at 4 °C. The beads were washed three times in 1 ml of TBS containing 0.1% Triton X-100 and then eluted with 250 μl of TBS containing 0.1% Triton X-100 and 200 mM *N*-acetylglucosamine. The presence of comparable amounts of DG protein in each elution was confirmed via Western blot analysis with DG antibodies, as described above.

To immunoprecipitate α-DG from mouse tissues, mouse brains or eyes were homogenized in TBS with a proteinase inhibitor mixture and then solubilized with 1% Triton X-100. Samples were centrifuged at 15,000 rpm for 10 min, and then the supernatants were incubated with or without anti-α-DG core protein (25). α-DG was immunoprecipitated using protein G beads. The α-DG-protein G beads were washed with TBS containing 0.1% Triton X-100 three times and then tested for binding with PikaLG, as described above.

Heparin Affinity Beads—PikaLG-containing cell lysates were incubated with the heparin beads (Sigma) overnight at 4 °C. After three washes with TBS containing 0.1% Nonidet P-40, bound materials were eluted with SDS-sample buffer.

Immunofluorescent Staining—Mouse eye cups were fixed in 4% paraformaldehyde/phosphate-buffered saline (PBS) for 30 min. Samples were cryoprotected, embedded, frozen, and sectioned 20 μm thick. Slides were incubated with blocking solution (5% normal goat serum and 0.5% Triton X-100 in PBS) for 1 h. Sections were incubated with primary antibodies at room temperature for 4 h, washed with PBS for 10 min, and incubated with secondary antibodies for 2 h. The sections were coverslipped with Gelvatol after rinsing with 0.02% Triton X-100 in PBS.

Quantitative Real Time PCR Analysis—Total RNA (1 μg) from the mouse retina was isolated using TRIzol reagent (Invitrogen) and converted to cDNA using Superscript II RTase (Invitrogen). Quantitative real time PCR was performed using SYBR Green ER qPCR Super MIX (Invitrogen) and the Thermal Cycler Dice Real Time System single MRQ TP870 (Takara) according to the manufacturer's instructions. Quantification was performed using Thermal Cycler Dice Real Time System software version 2.0 (Takara). Primers used in gene amplification were as follows: amplification of the pikachurin gene, Pikachurin-F, GGAAGATTACAGTGGATGACTACG, and Pikachurin-R, GTGTGCAGAGCGATTTCCTTCATTC; amplification of β-actin gene, actin-F, CGTGCGTGACATCAAAGAGAA, and actin-R, TGGATGCCACAGGATTCCAT.

RESULTS

Properties of the Pikachurin-Dystroglycan Interaction—To analyze binding between pikachurin and α-DG, we used recombinant pikachurin LG domains with a myc-His tandem tag (PikaLG) and α-DG fused to an Fc tag (DGFc) (Fig. 1*A*) (22). Previous data suggest that the pikachurin-DG interaction requires divalent cations (22). To further characterize this requirement, we analyzed PikaLG-DGFc binding in the presence of Ca^{2+}, Mg^{2+}, or Mn^{2+} using a pulldown assay (Fig. 1*B*). Ca^{2+} produced the strongest binding, whereas Mn^{2+} gave only faint binding, and no binding was observed with Mg^{2+} alone. To evaluate PikaLG-DGFc binding quantitatively, we developed a solid-phase binding assay. DGFc was immobilized on microplates, and cell lysates containing PikaLG were applied for binding. Signals representing binding of PikaLG to DGFc were detected, whereas no detectable signal was obtained from mock-transfected cell lysates (supplemental Fig. 1). Immobilized Fc protein showed no difference in signal intensity between PikaLG-containing and mock-transfected cell lysates, confirming the lack of specific interactions through the Fc portion (supplemental Fig. 1). We concluded that the solid-phase binding assay is sufficient to quantitatively detect PikaLG-DGFc interactions. The solid-phase binding assays showed results comparable with the pulldown assays. We observed a reduction in binding of around 70% in the presence of Mn^{2+} and a strong reduction in the presence of Mg^{2+}, similar to that seen in the presence of EDTA for chelation of divalent cations (Fig. 1*C*). The solid-phase binding assays in various Ca^{2+} concentrations established that the concentration required for half-maximal binding is ~80 μM (Fig. 1*D*). It has been reported that heparin or a high NaCl concentration (0.5 M) inhibits binding of laminin-111 and agrin to α-DG (27, 28). We examined the effects of heparin and NaCl on PikaLG-DGFc binding. The results showed that PikaLG-DGFc binding was inhibited slightly at 0.5 M NaCl (~80% binding), and the inhibitory effect

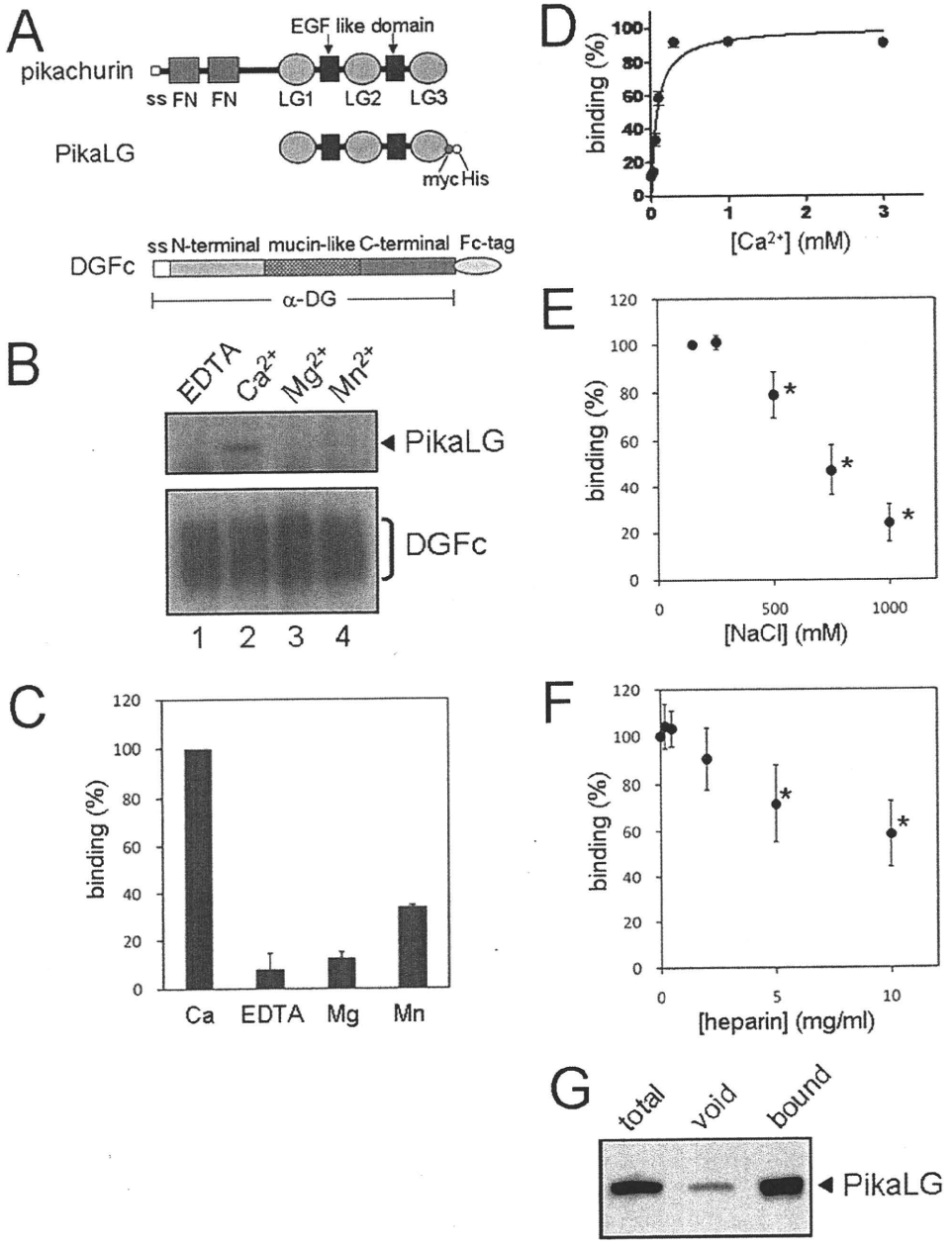

FIGURE 1. **Biochemical characterization of pikachurin-dystroglycan interaction.** *A*, schematic representation of recombinant pikachurin and α-DG. Pikachurin contains a signal sequence (*ss*), two fibronectin 3 (*FN*) domains, three laminin globular (*LG*) domains, and two calcium-binding EGF-like (*EGF like*) domains. Recombinant pikachurin LG domains (*PikaLG*) contain amino acid residues 391–1071 and a tandem myc-His tag at the C terminus. α-DG contains the signal sequence (*ss*), N-terminal, mucin-like, and C-terminal domains. Recombinant α-DG (*DGFc*) has an Fc tag at the C terminus. *B*, divalent cation is necessary for pikachurin-dystroglycan interaction. PikaLG binding to DGFc-protein A beads was tested in the presence of 2 mM EDTA (*lane 1*) and 2 mM each of Ca^{2+} (*lane 2*), Mg^{2+} (*lane 3*), or Mn^{2+} (*lane 4*). Bound PikaLG was detected by Western blotting with an anti-His tag antibody (*upper panel*, indicated by PikaLG). Comparable amounts of DGFc proteins on protein A beads were confirmed by staining with an anti-Fc antibody (*lower panel*, indicated by DGFc). *C*, quantitative solid-phase binding assays for divalent cation dependence. PikaLG binding to immobilized DGFc was tested in the presence of 2 mM EDTA and 2 mM each of Ca^{2+}, Mg^{2+}, or Mn^{2+}. Binding in the presence of Ca^{2+} was set as 100%. Data shown are the average of three independent experiments with standard deviations. *D*, Ca^{2+}-dependent binding of pikachurin to dystroglycan. PikaLG binding to DGFc was tested in various Ca^{2+} concentrations by solid-phase binding assays. The binding data were fit to the equation $Y = B_{max}x/(K_d + x)$, where K_d is the concentration required to reach half-maximal binding, and B_{max} is maximal binding. Maximal binding was set as 100%. $K_d = 78 \pm 15$ μM. Data shown are the average of four independent experiments with standard deviations. *E* and *F*, effects of NaCl (*E*) and heparin (*F*) on the pikachurin-dystroglycan interaction. PikaLG binding to DGFc was tested in various NaCl or heparin concentrations by solid-phase binding assays. Binding in the presence of 150 mM NaCl (*E*) or in the absence of heparin (*F*) was set as 100%. Data shown are the average of four (*E*) and six (*F*) independent experiments with standard deviations. *, $p < 0.05$. *G*, binding of pikachurin LG domains to heparin. Lysates from PikaLG-expressing cells were incubated with heparin affinity beads. Total lysate sample (*total*, *lane 1*), flow-through (*void*, *lane 2*), and bound (*bound*, *lane 3*) fractions were analyzed by Western blotting with an antibody to anti-Myc tag.

increased with higher concentrations of NaCl (Fig. 1*E*). No significant inhibitory effect was detected with heparin at 2 mg/ml (Fig. 1*F*), which is a sufficient concentration to completely inhibit α-DG binding to laminin-111 or agrin (28, 29). At 10 mg/ml heparin, PikaLG-DGFc binding was reduced to 60% (Fig. 1*F*). We confirmed that these conditions (0.5 M NaCl and 2 mg/ml heparin) do inhibit laminin-111 binding to DGFc (data not shown). To examine whether PikaLG has heparin binding capacity, we exposed lysates prepared from PikaLG-expressing cells to heparin affinity beads (Fig. 1*G*). Binding of PikaLG to heparin affinity beads was positive, indicating that PikaLG contains a heparin-binding site.

Dissection of Domains Necessary for Pikachurin-Dystroglycan Interaction—All known DG ligand proteins (laminin-111, laminin-211, agrin, perlecan, and neurexin) contain LG domains, through which they bind to α-DG. Pikachurin contains three LG domains in its C terminus. To examine which LG domain serves as the α-DG-binding site, we constructed single or tandem LG domains (Fig. 2*A*) and examined DGFc binding to each construct. We confirmed expression of all constructs in cells and then tested cell lysates containing comparable amounts of each LG protein for binding to DGFc (Fig. 2*B*). We found that the LG2-LG3 tandem construct binds to DGFc at a level similar to that of the full-length construct (Fig. 2*B*, *right panel*, *lanes 5* and *6*). Binding of other constructs to DGFc was minimal or undetectable. Solid-phase binding assays also confirmed that LG2-3 bound to DGFc, whereas the other deletion constructs did not (Fig. 2*C*). When PikaLG deletion constructs were subjected to SDS gel electrophoresis without heat denaturing, the constructs containing LG1 domains appeared at higher molecular weights than observed with heat denaturing (Fig. 2*D*). This result indicates that pikachurin forms oligomeric structures. Al-

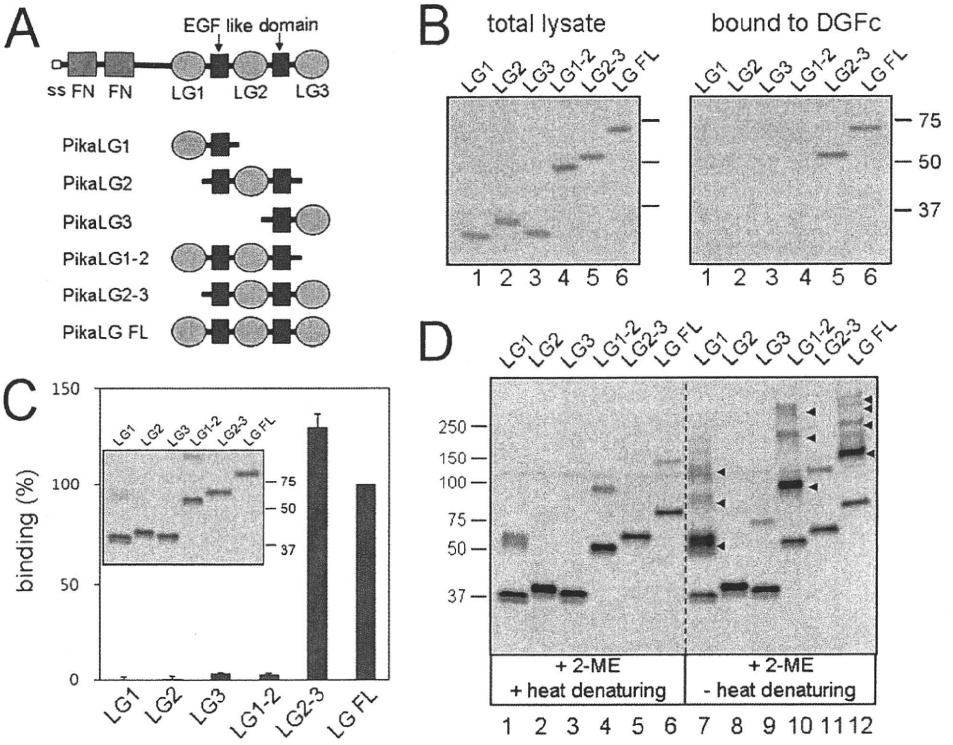

FIGURE 2. **Dissection of the dystroglycan binding region in pikachurin.** *A*, schematic representation of pikachurin deletion mutant proteins. All constructs contain a tandem myc-His tag at the C terminus. *ss*, signal sequence. *B*, binding of pikachurin deletion constructs to dystroglycan. Each deletion construct was expressed in HEK293 cells, and cell lysates were subjected to the DGFc binding assay. PikaLG in the reaction mixture (*left panel*) and PikaLG bound to DGFc-protein G-beads (*right panel*) were analyzed by Western blotting with an anti-Myc tag antibody. *C*, solid-phase binding assays for pikachurin deletion constructs. Cell lysates containing comparable amounts of each deletion construct were tested for DGFc binding. Binding of full-length DGFc was set as 100%. Data shown are the average of four independent experiments with standard deviations. *Inset*, Western blot analysis to confirm the amount of each LG protein used in the binding assays. *D*, oligomer formation of pikachurin. Cell lysates containing comparable amounts of each construct were dissolved in SDS sample buffer containing 2-mercaptoethanol (*2-ME*) and then subjected to SDS-PAGE with (*+2-ME, +heat denaturing*) or without (*+2-ME, −heat denaturing*) heat denaturing (95 °C, 5 min). Constructs containing LG1 (*LG1*, *LG1-2*, and *LG FL*) showed several higher molecular weight bands (*arrowheads*), which might indicate oligomeric structure formation by pikachurin.

though we observed no positive effect of the LG1 domain on PikaLG-DGFc binding, LG1-mediated oligomerization might play a physiological role in a more native situation. Overall, our results indicate that a certain steric structure formed by the LG2 and the LG3 domains is necessary for the pikachurin-DG interaction.

LARGE plays a crucial role in the DG modification process (17, 30). For LARGE-dependent modification of α-DG, two distinct domains of α-DG, the N-terminal domain and the first half of the mucin-like domain, are necessary. The N-terminal domain of α-DG is recognized by LARGE during post-translational maturation of DG and then proteolytically removed. The first half of the mucin-like domain of α-DG is modified with certain glycans necessary for acquiring ligand binding activity (30). To investigate whether these domains of α-DG are required for pikachurin binding, we used several DGFc deletion constructs (Fig. 3*A*). DG-N, which contains only the N-terminal domain, did not bind to PikaLG (Fig. 3*B*, *lane 2*). DGΔN, which lacks the N-terminal domain, also failed to bind to PikaLG, even though it contains the entire mucin-like domain (Fig. 3*B*, *lane 3*). Co-expression with LARGE enhanced PikaLG binding to full-length DGFc (DG-wt) (Fig. 3*B*, *lanes 4* and *5*). Using deletion constructs lacking the C-terminal domain (DGΔC) or containing the N-terminal domain plus the first half of the mucin-like domain (and DG^{half}), we showed that pikachurin-binding domains are located within the first half of the mucin-like domain (Fig. 3*C*). We examined binding of laminin-111 to these constructs using an overlay assay and confirmed that PikaLG binds to the same constructs that are able to capture laminin-111 (Fig. 3, *B* and *C*, *bottom panels*).

Disruption of Pikachurin Binding and Localization in Dystroglycanopathy Animals—We investigated various aspects of the pikachurin-DG interaction in dystroglycanopathy model animals. First, we used *POMGnT1*-deficient mice to investigate whether the GlcNAc-β1, 2-branch on *O*-Man is necessary for pikachurin binding. Endogenous α-DG was immunoprecipitated from brain extracts of *POMGnT1*-deficient and littermate heterozygous mice using antibodies that recognize the α-DG core protein (AP-G074). Precipitates were then incubated with lysates prepared from PikaLG-expressing cells (Fig. 4*A*). Western blot analysis of the immunoprecipitated materials confirmed that α-DG from the *POMGnT1*-deficient samples was hypoglycosylated, as evidenced by reduced molecular size. Whereas PikaLG bound to control α-DG of normal molecular size, the PikaLG-α-DG interaction was dramatically reduced in *POMGnT1*-deficient mice.

Next, we examined whether native α-DG from $Large^{myd}$ (myd) mice binds to pikachurin. Endogenous α-DG was immunoprecipitated from brains of myd or control heterozygous mice and then tested for pikachurin binding (Fig. 4*B*). We observed PikaLG binding to control α-DG with normal molecular size but not to hypoglycosylated α-DG from the myd mouse brain.

We also examined the PikaLG binding to native α-DG prepared from these mutant mice brains by solid-phase assays. Although binding signals obtained from the native DG preparations were generally weaker than those of DGFc, Ca^{2+}-sensitive binding was detected in control heterozygous samples (Fig. 4*C*). However, no significant binding was detected in mutant samples. These data indicate that the pikachurin-DG interaction is disrupted in dystroglycanopathy animals.

We also examined pikachurin expression and localization in the ribbon synapses of *POMGnT1*-deficient and myd mice.

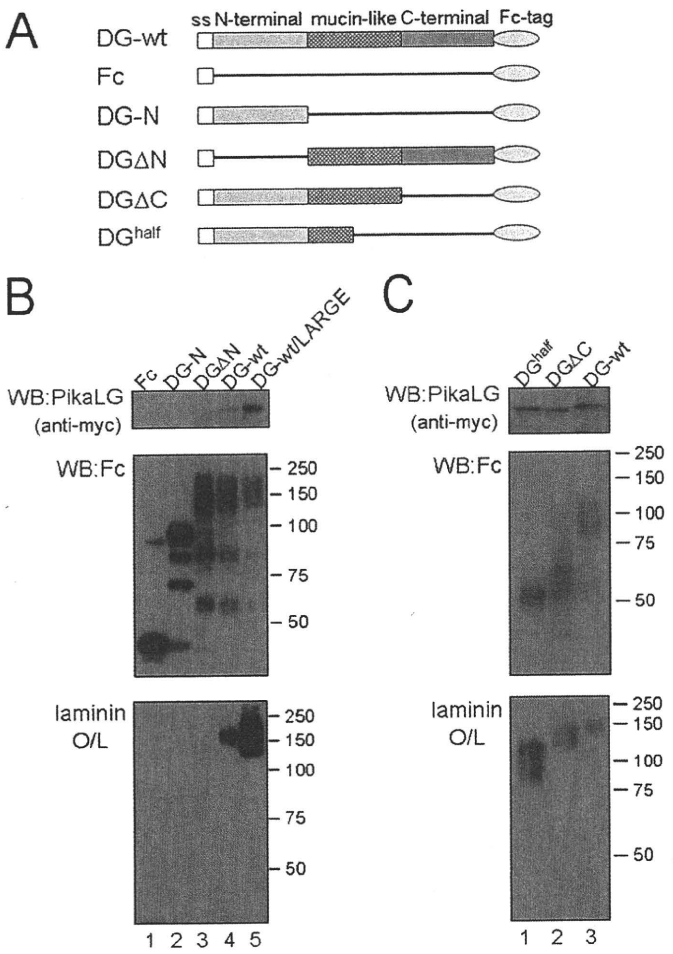

FIGURE 3. **Dystroglycan functional domains for pikachurin binding.** *A*, schematic representation of deletion mutants of DGFc proteins. *ss*, signal sequence. *B* and *C*, dissection of dystroglycan domains necessary for pikachurin binding. Each deletion construct was expressed in HEK293 cells and recovered from the culture media using protein A beads. The DG-wt construct was expressed without or with LARGE (*B*, *lanes 4* and *5*). Lysates from PikaLG-expressing cells were subjected to protein A beads that had captured each DGFc mutant protein. PikaLG binding was detected by Western blotting with an anti-Myc antibody (*upper panel, PikaLG*). Comparable amounts of DGFc mutant proteins on protein A beads were confirmed by Western blotting (*WB*) with an anti-Fc antibody (*middle panel, Fc*). The blot was also tested using a laminin-111 overlay assay (*bottom panel*, laminin *O/L*).

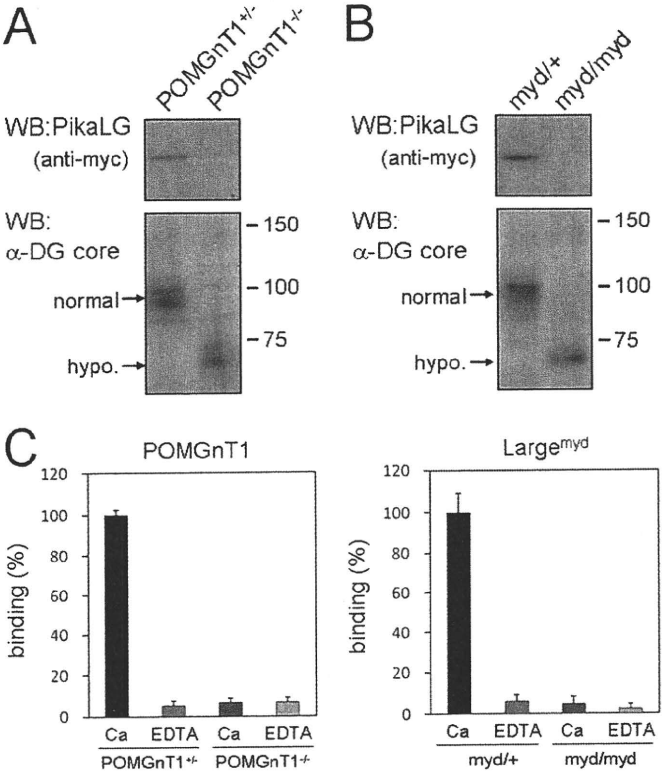

FIGURE 4. **Reduced pikachurin binding to α-dystroglycan in dystroglycanopathy animals.** α-DG was immunoprecipitated from the brains of *POMGnT1*-deficient (*A*) and *Large*^{myd} (*B*) mice. Littermates were used as controls. Lysates from PikaLG-expressing cells were incubated with the immunoprecipitated materials to examine PikaLG-DG binding. PikaLG binding was detected by Western blotting (*WB*) with an anti-Myc antibody (*upper panel, PikaLG*). Comparable amounts of α-DG were confirmed by Western blotting with anti-α-DG antibody (*lower panel, α-DG core*). Normal and hypoglycosylated (*hypo.*) sizes of α-DG are indicated on the *left side* of the blots. *C*, quantitative solid-phase binding assays for brain DG. Wheat germ agglutinin-enriched brain DG preparations from *POMGnT1*-deficient, *Large*^{myd}, and their littermates were immobilized and tested for PikaLG binding. Binding to DG preparations from littermate controls in the presence of Ca^{2+} was set as 100%. Data shown are the average of three individual preparations with standard deviations.

Immunofluorescence staining showed reduced pikachurin immunoreactivity in the ribbon synapse of *POMGnT1*-deficient mice, as compared with littermate heterozygous controls (Fig. 5*A*). Immunostaining of β-DG showed no apparent difference in DG protein expression between *POMGnT1*-heterozygous and *POMGnT1*-deficient animals. Binding assays confirmed that pikachurin binding is reduced in *POMGnT1*-deficient eye tissue (Fig. 5*B*). The reduced signal intensity for normal size α-DG in eye tissue relative to that in brain tissue (Fig. 4) is likely due to a lower abundance of DG proteins in the eye. Immunostaining in myd mice showed severely reduced pikachurin immunoreactivity in the ribbon synapse (Fig. 5*C*). Binding assays confirmed that pikachurin binding is also reduced in myd eye tissue (Fig. 5*D*). Real time quantitative PCR analysis showed that the amount of the pikachurin transcript was unchanged in dystroglycanopathy models (supplemental Fig. 2). Endogenous pikachurin protein has not been detected by Western blotting, possibly due to low abundance and/or insolubility. These data demonstrate that pikachurin binding activity of α-DG is necessary for proper localization of pikachurin in the ribbon synapse.

DISCUSSION

In this study, we have characterized the pikachurin-DG interaction and demonstrated that both the GlcNAc-β1, 2-branch and LARGE-dependent modification on *O*-Man of α-DG are necessary for the interaction to occur. Defects in these modifications result in reduced pikachurin-DG binding and disruption of pikachurin localization in the ribbon synapse, which might provide a molecular explanation for the abnormal ERG observed in dystroglycanopathy (supplemental Fig. 3).

The earlier studies have shown that binding of ligand proteins to α-DG is Ca^{2+}-dependent (27, 28, 31). A crystal structure study revealed that the laminin α2-chain LG5 contains two Ca^{2+}-coordinating residues, Asp-2982 and Asp-3055. Other LG domains in α-DG ligand proteins commonly contain residues equivalent to these two residues (32). Sequence alignment revealed that each of the three LG domains in pikachurin con-

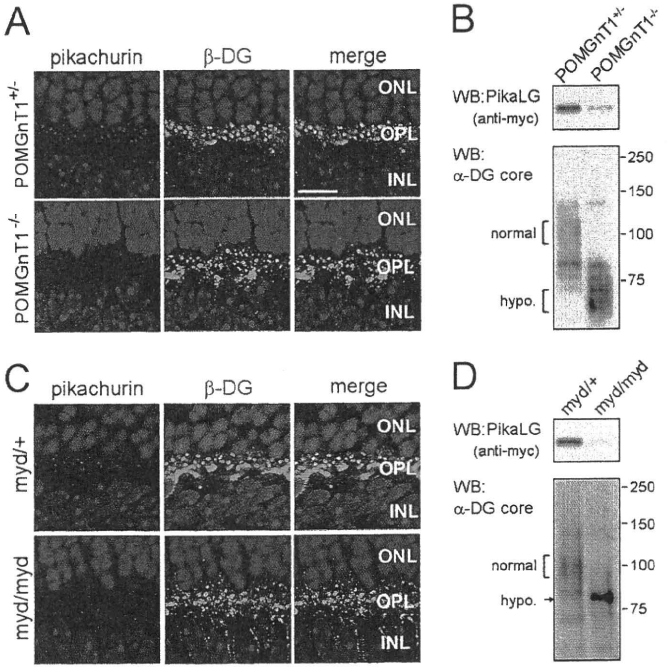

FIGURE 5. **Disruption of pikachurin localization in dystroglycanopathy animals.** *A* and *C*, immunofluorescence analysis of pikachurin in the outer plexiform layer (*OPL*). Retinal sections of *POMGnT1*-deficient (−/−) and *Large*^{myd} (myd/myd) mice, and their littermate heterozygous controls, were immunostained using antibodies to pikachurin (*red, left panels*) or β-DG (*green, middle panels*). Nuclei were stained with DAPI (*blue*). Merged images are shown in the *right panels*. *Scale bar*, 10 μm. *ONL*, outer nuclear layer; *INL*, inner nuclear layer. *B* and *D*, reduced pikachurin binding to α-DG in dystroglycanopathy models. α-DG was immunoprecipitated from eyes of *POMGnT1*-deficient (−/−) and *Large*^{myd} (myd/myd) mice, and their littermate heterozygous controls. PikaLG-containing cell lysates were incubated with the immunoprecipitated materials to examine PikaLG-DG binding. PikaLG binding was detected by Western blotting (*WB*) with anti-Myc antibody (*upper panel, PikaLG*). Comparable amounts of α-DG were confirmed by Western blotting with anti-α-DG antibody (*lower panel, α-DG core*). Normal and hypoglycosylated (*hypo.*) sizes of α-DG are indicated on the *left side* of the blots.

tains an Asp residue equivalent to Asp-2982 in the laminin α2-chain LG5, but they lack a residue equivalent to Asp-3055 (supplemental Fig. 4). The residue equivalent to Asp-3055 in pikachurin LG3 is Asn, which is capable of coordinating a Ca^{2+}, but LG1 and LG2 appear to lack the second Ca^{2+}-coordinating site. It has been shown that a single LG domain is usually insufficient for α-DG binding except laminin α1-chain LG4. This is also the case for pikachurin (Fig. 2). Thus, the adjacent tandem LG2-LG3 domains likely allow multiple Ca^{2+} sites to form a stable pikachurin-DG connection, as is proposed for other known ligand proteins (32). Interestingly, our data show that pikachurin can form oligomeric structures. This suggests the possibility that multimerization or clustering effects may play a role in modulating pikachurin-DG interactions in the native environment.

Unlike the laminin α1-chain and agrin (28, 29), the interaction of pikachurin with α-DG was relatively less sensitive to the inhibitory effects of heparin, although pikachurin LG domains have heparin binding capacity (Fig. 1). Heparin insensitivity at the submilligram/ml range is also observed with the laminin α2-chain and perlecan (33). These data may indicate that the α-DG-binding site is spatially distinct from the heparin-binding site in pikachurin LG domains, thus preventing heparin interference with the α-DG interaction. More interestingly, whereas 0.5 M NaCl strongly inhibits interaction between α-DG and other ligand proteins (33), only a modest inhibitory effect was observed for 0.5 M NaCl with pikachurin-DG binding. The strong inhibitory effects of NaCl on other DG ligand proteins indicate that, in addition to Ca^{2+}-mediated contact, an electrostatic effect may contribute partially to DG-ligand interactions. However, this may not be the case for pikachurin. Rather, it is likely that the Ca^{2+}-binding site in pikachurin primarily ensures the interaction with α-DG. There seem to be subtle differences between the binding of pikachurin to α-DG and that described for other LG domain proteins. Our ligand competition experiments show that PikaLG inhibits laminin-111 binding to DGFc, but even very high concentrations of laminin-111 do not inhibit PikaLG-binding to DGFc (supplemental Fig. 5). These data suggest that pikachurin might contain more binding sites on α-DG than does laminin-111. Alternatively, PikaLG might have much higher affinity for α-DG compared with laminin-111. Further investigation is necessary to reveal pikachurin-binding sites on α-DG in the future.

It is known that certain glycosylation events are necessary for α-DG ligand binding activity; however, the exact glycan structure necessary for the ligand binding is still not determined. Several lines of evidence have shown that among heterogeneous glycans on α-DG, *O*-mannosylation is an essential post-translational modification. The POMT1/2 complex catalyzes the initial Man transfer to Ser/Thr residues (9), and POMGnT1 synthesizes the GlcNAc-β1,2-branch on *O*-Man (12). A very recent study demonstrated the involvement of LARGE in the synthesis of phosphodiester-linked glycan on *O*-Man, which would serve as a laminin-binding moiety (13). Another study showed that β3GnT1 is involved in LARGE-dependent modification (34). β3GnT1 interacts with LARGE, and reduced expression of β3GnT1 leads to diminished synthesis of laminin-binding glycans. Here we have demonstrated that post-translational modification on *O*-Man mediated by LARGE and POMGnT1 is necessary for the pikachurin-DG interaction.

Mutations in these glycosylation pathways are causative for dystroglycanopathy, which is frequently associated with eye involvement, including abnormal retinal physiology. Several models for dystroglycanopathy, including *POMGnT1*-deficient, *Large*-mutant *Large*^{myd}, and *Large*^{vls} mice, show abnormal retinal physiology such as attenuation or delay in the electroretinogram b-wave (23, 24, 35). Previously, we reported that genetic disruption of pikachurin causes an ERG abnormality similar to those seen in other dystroglycanopathy model mice (22). In the retina, DG is expressed in the Müller glial end feet at the inner limiting membrane, in the glial end feet abutting the vasculature (36), and at ribbon synapses of photoreceptors in the outer plexiform layer (37–40). On the other hand, pikachurin localization is specific to the synaptic cleft of the photoreceptor ribbon synapse in the outer plexiform layer (22). In this study, we demonstrated that the pikachurin-DG interaction and pikachurin localization at the ribbon synapse are both disrupted in dystroglycanopathy animals. We propose that proper localization of pikachurin at the ribbon synapse, which is supported by functionally mature DG, plays important roles in the physiology of the retina.

Another physiological role of DG in the retina, apart from the ribbon synapse, was recently demonstrated (7). In that study, it has been shown that deletion of DG in the central nervous system (CNS) causes attenuation of the b-wave, which is associated with a selective loss of dystrophin and Kir4.1 clustering in glial end feet. Dystrophin is the product of the causative gene for Duchenne and Becker muscular dystrophies; it forms a protein complex with DG termed the dystrophin-glycoprotein complex. Loss of either dystrophin or DG results in reduction of the entire dystrophin-glycoprotein complex from the cell surface membrane (2, 41). Importantly, abnormalities in ERG similar to those seen in CNS-selective DG-deficient mice are frequently observed in individuals with Duchenne/Becker muscular dystrophy (42, 43). Dystrophin isoforms generated through differential promoter usage and alternative splicing are regulated in a tissue-specific and developmental manner. Dp260, which is transcribed using an internal promoter, is a retina-specific isoform located in the outer plexiform layer (44). In Dp260-disrupted mice, DG expression in the outer plexiform layer is severely reduced, and the implicit time of the b-wave is prolonged (45). These changes are also observed in dystroglycanopathy and pikachurin-deficient mouse models. Combined with our present work, these studies support the hypothesis that DG contributes to retina function via multiple mechanisms (7), including the pikachurin-DG-Dp260 molecular complex at the ribbon synapse and the DG-dystrophin-Kir4.1 clusters at glial end feet. Overall, our data not only shed light on the molecular pathogenesis of eye abnormalities in muscular dystrophy patients but also contribute to understanding the molecular mechanisms for ribbon synapse formation and maintenance.

Acknowledgments—We thank past and present members of the Toda laboratory for fruitful discussions and scientific contributions. We also thank Chiyomi Ito for technical support and Dr. Jennifer Logan for help with editing the manuscript.

REFERENCES

1. Barresi, R., and Campbell, K. P. (2006) *J. Cell. Sci.* **119,** 199–207
2. Cohn, R. D., Henry, M. D., Michele, D. E., Barresi, R., Saito, F., Moore, S. A., Flanagan, J. D., Skwarchuk, M. W., Robbins, M. E., Mendell, J. R., Williamson, R. A., and Campbell, K. P. (2002) *Cell* **110,** 639–648
3. Han, R., Kanagawa, M., Yoshida-Moriguchi, T., Rader, E. P., Ng, R. A., Michele, D. E., Muirhead, D. E., Kunz, S., Moore, S. A., Iannaccone, S. T., Miyake, K., McNeil, P. L., Mayer, U., Oldstone, M. B., Faulkner, J. A., and Campbell, K. P. (2009) *Proc. Natl. Acad. Sci. U.S.A.* **106,** 12573–12579
4. Michele, D. E., Kabaeva, Z., Davis, S. L., Weiss, R. M., and Campbell, K. P. (2009) *Circ. Res.* **105,** 984–993
5. Moore, S. A., Saito, F., Chen, J., Michele, D. E., Henry, M. D., Messing, A., Cohn, R. D., Ross-Barta, S. E., Westra, S., Williamson, R. A., Hoshi, T., and Campbell, K. P. (2002) *Nature* **418,** 422–425
6. Saito, F., Moore, S. A., Barresi, R., Henry, M. D., Messing, A., Ross-Barta, S. E., Cohn, R. D., Williamson, R. A., Sluka, K. A., Sherman, D. L., Brophy, P. J., Schmelzer, J. D., Low, P. A., Wrabetz, L., Feltri, M. L., and Campbell, K. P. (2003) *Neuron* **38,** 747–758
7. Satz, J. S., Philp, A. R., Nguyen, H., Kusano, H., Lee, J., Turk, R., Riker, M. J., Hernández, J., Weiss, R. M., Anderson, M. G., Mullins, R. F., Moore, S. A., Stone, E. M., and Campbell, K. P. (2009) *J. Neurosci.* **29,** 13136–13146
8. Chiba, A., Matsumura, K., Yamada, H., Inazu, T., Shimizu, T., Kusunoki, S., Kanazawa, I., Kobata, A., and Endo, T. (1997) *J. Biol. Chem.* **272,** 2156–2162
9. Manya, H., Chiba, A., Yoshida, A., Wang, X., Chiba, Y., Jigami, Y., Margolis, R. U., and Endo, T. (2004) *Proc. Natl. Acad. Sci. U.S.A.* **101,** 500–505
10. Beltrán-Valero de Bernabé, D., Currier, S., Steinbrecher, A., Celli, J., van Beusekom, E., van der Zwaag, B., Kayserili, H., Merlini, L., Chitayat, D., Dobyns, W. B., Cormand, B., Lehesjoki, A. E., Cruces, J., Voit, T., Walsh, C. A., van Bokhoven, H., and Brunner, H. G. (2002) *Am. J. Hum. Genet.* **71,** 1033–1043
11. van Reeuwijk, J., Janssen, M., van den Elzen, C., Beltran-Valero de Bernabé, D., Sabatelli, P., Merlini, L., Boon, M., Scheffer, H., Brockington, M., Muntoni, F., Huynen, M. A., Verrips, A., Walsh, C. A., Barth, P. G., Brunner, H. G., and van Bokhoven, H. (2005) *J. Med. Genet.* **42,** 907–912
12. Yoshida, A., Kobayashi, K., Manya, H., Taniguchi, K., Kano, H., Mizuno, M., Inazu, T., Mitsuhashi, H., Takahashi, S., Takeuchi, M., Herrmann, R., Straub, V., Talim, B., Voit, T., Topaloglu, H., Toda, T., and Endo, T. (2001) *Dev. Cell* **1,** 717–724
13. Yoshida-Moriguchi, T., Yu, L., Stalnaker, S. H., Davis, S., Kunz, S., Madson, M., Oldstone, M. B., Schachter, H., Wells, L., and Campbell, K. P. (2010) *Science* **327,** 88–92
14. Kobayashi, K., Nakahori, Y., Miyake, M., Matsumura, K., Kondo-Iida, E., Nomura, Y., Segawa, M., Yoshioka, M., Saito, K., Osawa, M., Hamano, K., Sakakihara, Y., Nonaka, I., Nakagome, Y., Kanazawa, I., Nakamura, Y., Tokunaga, K., and Toda, T. (1998) *Nature* **394,** 388–392
15. Brockington, M., Blake, D. J., Prandini, P., Brown, S. C., Torelli, S., Benson, M. A., Ponting, C. P., Estournet, B., Romero, N. B., Mercuri, E., Voit, T., Sewry, C. A., Guicheney, P., and Muntoni, F. (2001) *Am. J. Hum. Genet.* **69,** 1198–1209
16. Grewal, P. K., Holzfeind, P. J., Bittner, R. E., and Hewitt, J. E. (2001) *Nat. Genet.* **28,** 151–154
17. Barresi, R., Michele, D. E., Kanagawa, M., Harper, H. A., Dovico, S. A., Satz, J. S., Moore, S. A., Zhang, W., Schachter, H., Dumanski, J. P., Cohn, R. D., Nishino, I., and Campbell, K. P. (2004) *Nat. Med.* **10,** 696–703
18. Muntoni, F., Torelli, S., and Brockington, M. (2008) *Neurotherapeutics* **5,** 627–632
19. Godfrey, C., Clement, E., Mein, R., Brockington, M., Smith, J., Talim, B., Straub, V., Robb, S., Quinlivan, R., Feng, L., Jimenez-Mallebrera, C., Mercuri, E., Manzur, A. Y., Kinali, M., Torelli, S., Brown, S. C., Sewry, C. A., Bushby, K., Topaloglu, H., North, K., Abbs, S., and Muntoni, F. (2007) *Brain* **130,** 2725–2735
20. Lisi, M. T., and Cohn, R. D. (2007) *Biochim. Biophys. Acta* **1772,** 159–172
21. Sigesmund, D. A., Weleber, R. G., Pillers, D. A., Westall, C. A., Panton, C. M., Powell, B. R., Héon, E., Murphey, W. H., Musarella, M. A., and Ray, P. N. (1994) *Ophthalmology* **101,** 856–865
22. Sato, S., Omori, Y., Katoh, K., Kondo, M., Kanagawa, M., Miyata, K., Funabiki, K., Koyasu, T., Kajimura, N., Miyoshi, T., Sawai, H., Kobayashi, K., Tani, A., Toda, T., Usukura, J., Tano, Y., Fujikado, T., and Furukawa, T. (2008) *Nat. Neurosci.* **11,** 923–931
23. Lee, Y., Kameya, S., Cox, G. A., Hsu, J., Hicks, W., Maddatu, T. P., Smith, R. S., Naggert, J. K., Peachey, N. S., and Nishina, P. M. (2005) *Mol. Cell. Neurosci.* **30,** 160–172
24. Liu, J., Ball, S. L., Yang, Y., Mei, P., Zhang, L., Shi, H., Kaminski, H. J., Lemmon, V. P., and Hu, H. (2006) *Mech. Dev.* **123,** 228–240
25. Kanagawa, M., Nishimoto, A., Chiyonobu, T., Takeda, S., Miyagoe-Suzuki, Y., Wang, F., Fujikake, N., Taniguchi, M., Lu, Z., Tachikawa, M., Nagai, Y., Tashiro, F., Miyazaki, J., Tajima, Y., Takeda, S., Endo, T., Kobayashi, K., Campbell, K. P., and Toda, T. (2009) *Hum. Mol. Genet.* **18,** 621–631
26. Miyagoe-Suzuki, Y., Masubuchi, N., Miyamoto, K., Wada, M. R., Yuasa, S., Saito, F., Matsumura, K., Kanesaki, H., Kudo, A., Manya, H., Endo, T., and Takeda, S. (2009) *Mech. Dev.* **126,** 107–116
27. Ervasti, J. M., and Campbell, K. P. (1993) *J. Cell Biol.* **122,** 809–823
28. Gee, S. H., Montanaro, F., Lindenbaum, M. H., and Carbonetto, S. (1994) *Cell* **77,** 675–686
29. Ervasti, J. M., Burwell, A. L., and Geissler, A. L. (1997) *J. Biol. Chem.* **272,** 22315–22321
30. Kanagawa, M., Saito, F., Kunz, S., Yoshida-Moriguchi, T., Barresi, R., Kobayashi, Y. M., Muschler, J., Dumanski, J. P., Michele, D. E., Oldstone, M. B., and Campbell, K. P. (2004) *Cell* **117,** 953–964
31. Sugita, S., Saito, F., Tang, J., Satz, J., Campbell, K., and Südhof, T. C. (2001)

J. Cell Biol. **154,** 435–445
32. Hohenester, E., Tisi, D., Talts, J. F., and Timpl, R. (1999) *Mol. Cell* **4,** 783–792
33. Talts, J. F., Andac, Z., Göhring, W., Brancaccio, A., and Timpl, R. (1999) *EMBO J.* **18,** 863–870
34. Bao, X., Kobayashi, M., Hatakeyama, S., Angata, K., Gullberg, D., Nakayama, J., Fukuda, M. N., and Fukuda, M. (2009) *Proc. Natl. Acad. Sci. U.S.A.* **106,** 12109–12114
35. Holzfeind, P. J., Grewal, P. K., Reitsamer, H. A., Kechvar, J., Lassmann, H., Hoeger, H., Hewitt, J. E., and Bittner, R. E. (2002) *Hum. Mol. Genet.* **11,** 2673–2687
36. Montanaro, F., Carbonetto, S., Campbell, K. P., and Lindenbaum, M. (1995) *J. Neurosci. Res.* **42,** 528–538
37. Blank, M., Koulen, P., and Kröger, S. (1997) *J. Comp. Neurol.* **389,** 668–678
38. Koulen, P., Blank, M., and Kröger, S. (1998) *J. Neurosci. Res.* **51,** 735–747
39. Blank, M., Koulen, P., Blake, D. J., and Kröger, S. (1999) *Eur. J. Neurosci.* **11,** 2121–2133
40. Jastrow, H., Koulen, P., Altrock, W. D., and Kröger, S. (2006) *Invest. Ophthalmol. Vis. Sci.* **47,** 17–24
41. Ohlendieck, K., and Campbell, K. P. (1991) *J. Cell. Biol.* **115,** 1685–1694
42. Cibis, G. W., Fitzgerald, K. M., Harris, D. J., Rothberg, P. G., and Rupani, M. (1993) *Invest. Ophthalmol. Vis. Sci.* **34,** 3646–3652
43. Pillers, D. A., Fitzgerald, K. M., Duncan, N. M., Rash, S. M., White, R. A., Dwinnell, S. J., Powell, B. R., Schnur, R. E., Ray, P. N., Cibis, G. W., and Weleber, R. G. (1999) *Hum. Genet.* **105,** 2–9
44. D'Souza, V. N., Nguyen, T. M., Morris, G. E., Karges, W., Pillers, D. A., and Ray, P. N. (1995) *Hum. Mol. Genet.* **4,** 837–842
45. Kameya, S., Araki, E., Katsuki, M., Mizota, A., Adachi, E., Nakahara, K., Nonaka, I., Sakuragi, S., Takeda, S., and Nabeshima, Y. (1997) *Hum. Mol. Genet.* **6,** 2195–2203

Defective glycosylation of α-dystroglycan contributes to podocyte flattening

Kenichiro Kojima[1], Hitonari Nosaka[1], Yuki Kishimoto[1], Yuri Nishiyama[1], Seiichi Fukuda[1], Masaru Shimada[1], Kenzo Kodaka[1], Fumiaki Saito[2], Kiichiro Matsumura[2], Teruo Shimizu[2], Tatsushi Toda[3], Satoshi Takeda[4], Hiroshi Kawachi[5] and Shunya Uchida[1]

[1]Department of Internal Medicine, Teikyo University School of Medicine, Tokyo, Japan; [2]Department of Neurology and Neuroscience, Teikyo University School of Medicine, Tokyo, Japan; [3]Division of Clinical Genetics, Department of Medical Genetics, Osaka University Graduate School of Medicine, Osaka, Japan; [4]Otsuka GEN Research Institute, Otsuka Pharmaceutical, Tokushima, Japan and [5]Institute of Nephrology, Niigata University, Niigata, Japan

In addition to skeletal muscle and the nervous system, α-dystroglycan is found in the podocyte basal membrane, stabilizing these cells on the glomerular basement membrane. Fukutin, named after the gene responsible for Fukuyama-type congenital muscular dystrophy, is a putative glycosyltransferase required for the post-translational modification of α-dystroglycan. Chimeric mice targeted for both alleles of *fukutin* develop severe muscular dystrophy; however, these mice do not have proteinuria. Despite the lack of a functional renal defect, we evaluated glomerular structure and found minor abnormalities in the chimeric mice by light microscopy. Electron microscopy revealed flattening of podocyte foot processes, the number of which was significantly lower in the chimeric compared to wild-type mice. A monoclonal antibody against the laminin-binding carbohydrate residues of α-dystroglycan did not detect α-dystroglycan glycosylation in the glomeruli by immunoblotting or immunohistochemistry. In contrast, expression of the core α-dystroglycan protein was preserved. There was no statistical difference in dystroglycan mRNA expression or in the amount of nephrin and α3-integrin protein in the chimeric compared to the wild-type mice as judged by immunohistochemistry and real-time RT-PCR. Thus, our results indicate that appropriate glycosylation of α-dystroglycan has an important role in the maintenance of podocyte architecture.

Kidney International (2011) **79,** 311–316; doi:10.1038/ki.2010.403; published online 13 October 2010

KEYWORDS: adhesion molecule; dystroglycan; foot process; glycosylation; podocyte

Correspondence: *Kenichiro Kojima, Department of Internal Medicine, Teikyo University School of Medicine, 2-11-1 Kaga, Itabashi-ku, Tokyo 173-8605, Japan. E-mail: kojima@med.teikyo-u.ac.jp*

Received 26 January 2010; revised 12 August 2010; accepted 31 August 2010; published online 13 October 2010

Podocytes are highly differentiated cells that possess specialized projections called foot processes. Adhesion molecules of podocytes are likely to have an important role in the maintenance of podocyte morphology by anchoring of these cells to the glomerular basement membrane (GBM).[1,2] To date, two major adhesion protein systems have been identified. As the first step, $\alpha_3\beta_1$-integrin was localized exclusively to the podocyte basal membrane domains in normal and flattened human podocytes and was speculated to contribute to the firm adhesion of the podocytes to the GBM matrix proteins.[3–5]

Recently, α- and β-dystroglycans were discovered in podocytes, and were found to be localized to the podocytes basal membrane domain.[6,7] Dystroglycan is composed of a transmembrane, heterodimeric complex of α- and β-subunits that link the extracellular matrix to the cell cytoskeleton. Gene knockout experiments have not been helpful for understanding the role of dystroglycans in podocyte function, because knockout results in early embryonic death, long before kidney glomeruli develop, and because Reichert's membrane, the first canonical basement membrane produced by the embryo, is disorganized, and it fails to withstand the blood pressure of maternal circulation.[8]

Fukuyama-type congenital muscular dystrophy (FCMD), discovered in Japan, is a severe muscular dystrophy with central nervous system involvement.[9] Fukutin, named after the gene responsible for FCMD, is a putative glycosyltransferase required for post-translational modification of α-dystroglycan.[10,11]

Chimeric mice generated using embryonic stem cells targeted for both *fukutin* alleles develop severe muscular dystrophy associated with the defective glycosylation of α-dystroglycan.[12] In this study, we investigated fukutin-deficient chimeric mice to clarify the role of α-dystroglycan glycosylation for maintaining podocyte architecture.

RESULTS

Chimeric mice showed muscle weakness, were unable to walk in a straight line, and dragged their feet as previously described.[12]

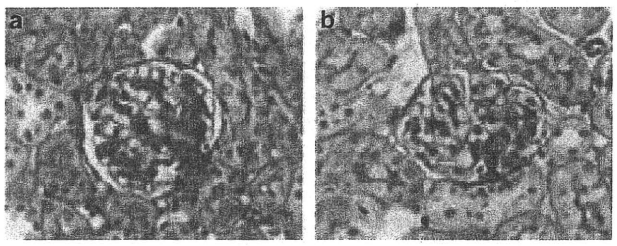

Figure 1 | Photomicrographs of periodic acid Schiff stain. Representative photomicrographs of wild-type (**a**) and the fukutin-deficient chimeric mice (**b**). Glomeruli from the fukutin-deficient chimeric mice have no abnormalities by light microscopy. Original magnification × 200.

Figure 2 | Transmitted electron photomicrograph of the fukutin-deficient chimeric mice. The flattening of foot processes was observed in segmental lesion of capillary lumens (arrowheads). No detachment of foot processes from the GBM was observed. Original magnification × 4000. GBM, glomerular basement membrane.

Light microscopy of kidney specimens showed minor abnormalities (Figure 1) together without massive albuminuria. Electron microscopy revealed morphological changes in podocytes such as vacuolization, microvillous transformation, and segmental foot process effacement. However, the detachment of foot processes from the GBM was not observed (Figure 2). The number of foot processes along the GBM decreased significantly in chimeric mice (1.39 ± 0.18/ μm GBM; Figure 3b) compared with wild-type mice (2.09 ± 0.01/μm GBM; Figure 3a) ($P = 0.039$; Figure 3c). In addition, the GBM was thickened and the three-layered structure of the GBM was lost under the lesion of flattened foot processes in chimeric mice (Figure 3b). The thickness of the GBM was increased significantly in chimeric mice (0.30 ± 0.03 μm) compared with wild-type mice (0.15 ± 0.01 μm) ($P = 0.043$; Figure 3d).

Immunohistochemistry using the IIH6 monoclonal antibody against the laminin-binding carbohydrate residues of α-dystroglycan (Figure 4a) and rabbit polyclonal antibody AP1530 against the 34 amino acids in the C-terminal domain of human α-dystroglycan indicated that the α-dystroglycan was localized along the glomerular capillary walls in a linear manner in wild-type mice kidneys (Figure 4c). In contrast, the expression of α-dystroglycan laminin-binding carbohydrate residues decreased in chimeric mice (Figure 4b). Immunohistochemistry revealed that expression of the core α-dystroglycan protein was relatively preserved in chimeric mice (Figure 4d).

In wild-type mice, immunoblotting detected a broad band around 150 kDa representing α-dystroglycan (Figure 4e). Expression of laminin-binding carbohydrate residues was reduced in chimeric mice (Figure 4e), whereas that of the core α-dystroglycan protein was relatively preserved in chimeric mice. An additional band around 75 kDa was detected in chimeric mice, suggesting that considerable parts of α-dystroglycan were hypoglycosylated (Figure 4f). There was no statistical difference in the mRNA expression of dystroglycan between the wild-type and chimeric mice (Figure 4g).

In wild-type mice, a laminin overlay assay detected a broad band around 150 kDa corresponding to α-dystroglycan, whereas the overlay assay revealed a deficiency in the laminin-binding activity of α-dystroglycan in chimeric mice (Figure 4h).

The expression of α_3-integrin (another adhesion molecule localized to the podocytes basal membrane domain) and nephrin (which is thought to be the main component of the slit diaphragm)[13] was also investigated. The expression levels of α_3-integrin and nephrin were unaltered in chimeric mice using immunohistochemistry and real-time RT-PCR (Figure 5a–d, g, and h).

Tetramethylrhodamine (TRITC)-conjugated wheat germ agglutinin (WGA) staining was performed to detect sialic acid and *N*-acetyl-glucosamine (GlcNAc) oligomer. WGA staining was observed along the glomerular capillary walls in a linear manner in wild-type mice. Similar staining was observed in chimeric mice, suggesting that fukutin deficiency did not affect GlcNAc oligomers and sialic acid (Figure 5e and f).

DISCUSSION

Dystroglycan is expressed in many cell types such as skeletal muscles, various epithelia, and in the nervous system.[14,15] α-Dystroglycan is heavily glycosylated by *O*-mannosyl glycosylation. It is speculated that α-dystroglycan carbohydrate residues are bound to the cationic LG domain common to several matrix proteins such as laminin and agrin.[16] In the glomerulus, α-dystroglycan is localized to basal cell membrane domains of the podocyte, stabilizes podocytes on the GBM, and presumably is involved in the pathogenesis of foot process flattening.[17]

Using the IIH6 monoclonal antibody, we found that the expression of α-dystroglycan laminin-binding carbohydrate residues decreased in fukutin-deficient chimeric mice, whereas expression of the core α-dystroglycan protein was preserved. These results confirmed that fukutin is involved in the modification of α-dystroglycan laminin-binding carbohydrate residues. We performed the laminin blot overlay assay to evaluate the binding activity of α-dystroglycan to laminin and revealed a severe reduction in the binding

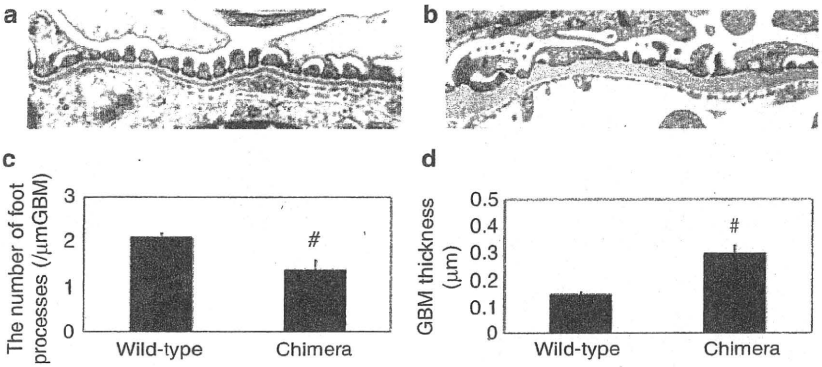

Figure 3 | The number of foot processes and the thickness of the GBM. Representative transmitted electron photomicrographs of wild-type (**a**) and the fukutin-deficient chimeric mice (**b**). The GBM under the foot process effacement is thickened and the three-layered structure is lost. The number of foot processes per μm GBM (**c**) and the thickness of the GBM (**d**) in wild-type mice (wild-type) and the chimeric mice (chimera). Values are expressed as means ± s.d. $^{\#}P<0.05$ vs wild type. GBM, glomerular basement membrane.

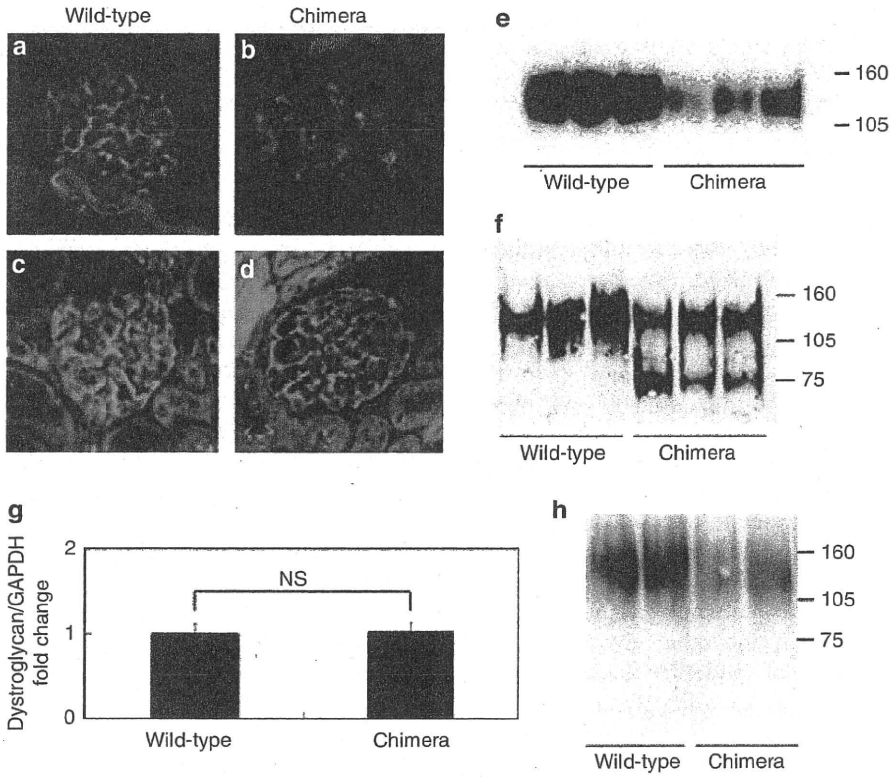

Figure 4 | Defective glycosylation of α-dystroglycan decreases the binding activity to laminin. Immunohistochemistry (**a–d**) and immunoblotting (**e, f**) reveal reduction of the laminin-binding carbohydrate residues of α-dystroglycan (**a, b, e**) in the chimeric mice (chimera) compared with the wild-type mice (wild-type). Expression of core protein of α-dystroglycan (**c, d, f**) is relatively preserved in the chimeric mice (chimera). The additional band around 75 kDa is detected in the chimeric mice, suggesting considerable parts of α-dystroglycan are hypoglycosylated (**f**). (**g**) Expression of dystroglycan by real-time RT-PCR in the wild-type mice (wild-type) and the chimeric mice (chimera). (**h**) Laminin binding activity of α-dystroglycan. Blot overlay analysis shows that the binding activity of α-dystroglycan is decreased in the chimeric mice (chimera). NS, not significant

activity in chimeric mice. Previously we reported that injury to α-dystroglycan with reactive oxygen species or protamine sulfate directly split the attachments of α-dystroglycan to laminin and agrin, and this led to the induction of foot process flattening.[17] Similar results were also found that for deglycosylated α-dystroglycan by reactive oxygen species, which led to impaired binding to laminin and agrin, and to foot process flattening.[18] These data suggest that defective glycosylation of α-dystroglycan causes inhibition of binding to laminin and agrin resulting in the flattening of foot processes.

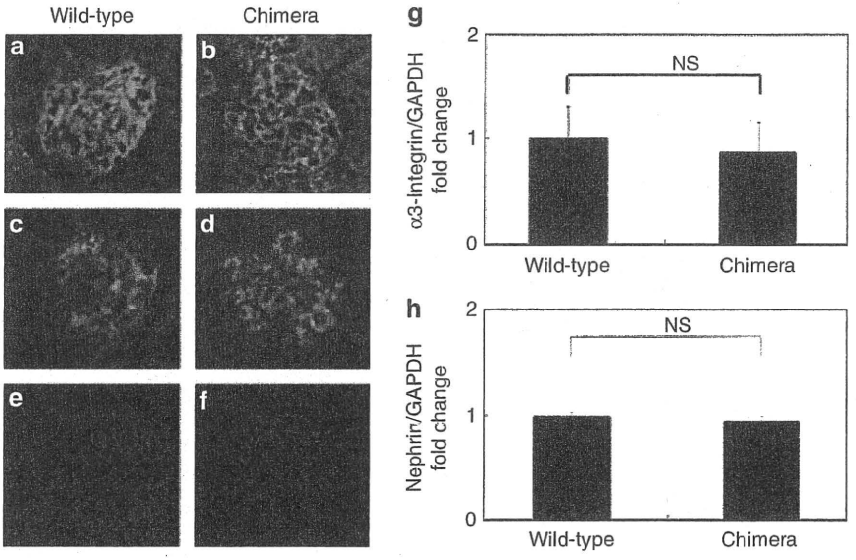

Figure 5 | Expression of α_3-integrin or nephrin, and WGA lectin staining. Immunohistochemistry (**a-d**) and real-time RT-PCR (**g, h**) for α_3-integrin (**a, b, g**) or nephrin (**c, d, h**), and TRITC-conjugated WGA lectin staining (**e, f**) in the wild-type mice (wild-type) or the chimeric mice (chimera). Expressions of α_3-integrin and nephrin are preserved in the chimeric mice (**b, d**). WGA staining is localized along the glomerular capillary walls in wild-type (**e**) and chimera (**f**). NS, not significant; TRITC, tetramethylrhodamine; WGA, wheat germ agglutinin.

The podocyte structure was changed in the fukutin-deficient chimeric mice. However, there was no detachment of foot processes from the GBM. The expression of α_3-integrin (another adhesion molecule localized to the podocyte basal membrane domain) was preserved in chimeric mice. Kitsiou *et al.*[19] found that anti-α_3-integrin monoclonal antibody decreased the adhesion of human podocytes to collagen type IV. Homozygous mutant mice with targeted knockout of α_3-integrin fail to form complete foot processes resulting in podocyte detachment.[20] The presence of α_3-integrin in chimeric mice might rescue the detachment of podocytes from the GBM.

WGA lectin staining was performed to detect sialic acid and GlcNAc oligomer in the glomerular capillaries. Sialic acid residues on podocalyxin and other glycoproteins are essential for maintenance of podocyte architecture.[21,22] Defect of heparan sulfate glycosaminoglycan containing GlcNAc oligomer is shown to induce foot process effacement without severe proteinuria.[23] WGA staining was retained in chimeric mice, suggesting that fukutin deficiency was not affecting glycosylation of other glycoproteins except for α-dystroglycan.

It is interesting to note that urinary protein excretion did not increase in chimeric mice despite the flattening of foot processes. One reason for this phenomenon may be that the degree of foot process effacement was not extensive. Furthermore, the expressions of α_3-integrin and nephrin were relatively preserved in chimeric mice. We reported decreased α_3-integrin expression and foot process effacement, which precedes the development of proteinuria, in puromycin aminonucleoside nephrosis.[5] In this study, the retained α_3-integrin might contribute to the prevention of proteinuria in chimeric mice. Nephrin, a member of the Ig superfamily, was first discovered as one of the slit diaphragm proteins.[13] Mutations in nephrin lead to a loss of normal podocyte structure, resulting in fetal proteinuria in congenital nephrotic syndrome of the Finnish type.[24,25] Some investigators have reported that nephrin expression is lower in patients with primary acquired nephrotic syndrome.[26,27] In this study, preserved α_3-integrin and nephrin might have prevented proteinuria in chimeric mice.

So far, no information is available concerning glomerular changes in FCMD in the literature, because these patients usually do not develop proteinuria. Most patients with FCMD develop serious muscle weakness, global developmental delay, and die by 20 years of age.[9] The lack of long-term survival might disturb development of proteinuria in FCMD patients. However, the possibility that foot process effacement occurs subtly in these patients during their infantile periods cannot be ruled out.

A generalized gene knockout of dystroglycan results in early embryonic death before the development of renal glomeruli[8] because the Reichiert's membrane matrix proteins are disorganized. Fukutin homozygous-null mice also cannot survive beyond an early embryonic stage because of the fragility of the basement membranes.[28] An example of dystroglycan function is observed in skeletal muscle cells where it mediates the redistribution of matrix proteins under the control of the actin cytoskeleton, and *vice versa*.[29] High-resolution electron microscopy showed that arrays of fibers in the lamina rara externa are irregularly arranged in puromycin aminonucleoside nephrosis and after protamine sulfate

perfusion.[17] Similar to that study, this study showed that chimeric mice had a significant increase in the thickness of the GBM with a loss of its three-layered structure. These findings imply that α-dystroglycan is important for organizing extracellular matrix proteins and forming a stable basement membrane structure in the glomerulus.

In conclusion, the results of this study indicate that appropriate glycosylation of α-dystroglycan may be important in the maintenance of podocyte architecture and matrix assembly in the GBM. Further investigation into the relationships of slit membrane-related molecules, cytoskeletal proteins, and adhesion molecules is essential to clarify the mechanisms of proteinuria.

MATERIALS AND METHODS

Antibodies and lectin

Mouse monoclonal antibodies against laminin-binding carbohydrate residues of α-dystroglycan (IIH6) were obtained from Upstate Biotechnology (Lake Placid, NY). Rabbit anti-laminin antibody was purchased from Sigma Chemical (St Louis, MO). Rabbit anti-human α_3-integrin polyclonal antiserum was obtained from Chemicon International (Temecula, CA). Preparations of rabbit polyclonal antibody against the 34 amino acids in the C-terminal domain of human α-dystroglycan (AP1530) and anti-nephrin antibody were described previously.[30,31] fluorescein isothiocyanate- or horseradish peroxidase-conjugated secondary antibodies were obtained from Dako (Glostrup, Denmark). TRITC-conjugated WGA was obtained from Vector Laboratories (Burlingame, PA).

Animals

Fukutin-deficient chimeric mice were generated using embryonic stem cells targeted for both *fukutin* alleles ($n=3$) as previously reported.[12] C57BL/6 mice were used as normal controls ($n=3$). Mice were killed at 7 months of age. All animal experiments were approved by the local ethics committee.

Urinary albumin excretion was determined using Albustix (Bayer Medical, Tokyo, Japan).

Light microscopy, immunochemistry, and lectin histochemistry

Renal cortices were fixed in 4% paraformaldehyde, embedded in paraffin, and 4 μm-thick sections were cut. Sections were stained with Periodic acid-Schiff reaction.

Frozen sections (4-μm thick) were cut and stained using the indirect immunofluorescence method. TRITC-conjugated WGA staining was performed according to the manufacturer's instructions.

Electron microscopy

The fixed renal cortices were embedded in epoxy resin using conventional methods. Ultrathin sections were prepared, stained with uranyl acetate and lead citrate, and were then examined with a JEOL 1200EX electron microscope (JEOL, Tokyo, Japan). To evaluate the morphological changes in podocytes, the number of epithelial foot processes per μm of GBM and thickness of GBM were calculated using a curvimeter. Three glomeruli were randomly selected from each mouse and 10 electron micrographs were taken in each glomerulus. Areas of wrinkled GBM were excluded. The measurements were taken from electron micrographs with magnifications of × 10,000.

Immunoblotting

Mouse kidney cortices were extracted with RIPA buffer (20 mM Tris-HCl, 150 mM NaCl, 2 mM EDTA, 1% Nonidet P-40, 1% sodium deoxycholate, 0.1% SDS) for 2 h at 4 °C, followed by centrifugation at 500 *g* for 5 min. The supernatants were dissolved in SDS sample buffer and electrophoresed on 7.5% polyacrylamide gels under reducing conditions. Gels loaded with samples were transferred onto nitrocellulose membranes (Amersham Pharmacia Biotech, Uppsala, Sweden). Immunoblotting was performed with the primary antibodies, and detection was performed with an enhanced chemiluminescence kit (Amersham Pharmacia Biotech).

Blot overlay analysis

The nitrocellulose transfers of renal cortex lysates were blocked in 10 mM Tris-HCl (pH 7.6), 140 mM NaCl, 1 mM $CaCl_2$, and 1 mM $MgCl_2$ (LBB) containing 5% non-fat dry milk for 1 h at room temperature. The transfers were incubated with LBB containing 0.1–0.5 μg per stripe EHS laminin (Koken, Tokyo, Japan) overnight at 4 °C. Bound laminin was detected using anti-laminin antibody and the development was conducted with an enhanced chemiluminescence kit (Amersham).

Real-time RT-PCR

RNA was isolated from renal tissues using TRIzol reagent (Invitrogen, Paisley, UK) according to the manufacturer's instructions. Total RNA (1 μg) was used as a template. Real-time RT-PCR was performed using the LightCycler FastStart kit with SYBR Green (Roche Molecular Systems, Alameda, CA). Reaction conditions were as follows: an initial hold at 50 °C for 10 min followed by 95 °C for 5 min to achieve first-strand synthesis. PCR was cycled for 40 iterations; 95 °C for 10 s, 55 °C for 30 s, and 72 °C for 1 min. The Reaction was completed at 72 °C for 10 min. The primer pairs used were: $\alpha_3\beta_1$-integrin (forward, TCCGTGGACATCGACTCTGA; reverse, AGCTTCATACAGGGCACGAG), dystroglycan (forward, GGACCCTGAGAAGAGCAGTG; reverse, TGGTAGGGAGGTGCATTAGG), nephrin (forward, GATCCAGGTCTCCGTCACTA; reverse, GAAGACCACCAACTGCAAAG). The transcript level in the wild-type was arbitrarily expressed as 1.

Statistics

All data are expressed as means ± s.d. Values were analyzed by unpaired Student's *t*-test. $P<0.05$ was considered significant.

DISCLOSURE

All the authors declared no competing interests.

REFERENCES

1. Kerjaschki D. Caught flat-footed: podocyte damage and the molecular bases of focal glomerulosclerosis. *J Clin Invest* 2001; **108**: 1583–1587.
2. Durvasula RV, Shankland SJ. Podocyte injury and targeting therapy: an update. *Curr Opin Nephrol Hypertens* 2006; **15**: 1–7.
3. Kerjaschki D, Ojha PP, Susani M *et al.* A β1-integrin receptor for fibronectin in human glomeruli. *Am J Pathol* 1989; **134**: 481–489.
4. Adler S. Characterization of glomerular epithelial cell matrix receptors. *Am J Pathol* 1992; **141**: 571–578.
5. Kojima K, Matsui K, Nagase M. Protection of α3 integrin-mediated podocyte shape by superoxide dismutase in the puromycin aminonucleoside nephrosis rat. *Am J Kidney Dis* 2000; **35**: 1175–1185.
6. Regele HM, Fillipovic E, Langer B *et al.* Glomerular expression of dystroglycans is reduced in minimal change nephrosis but not in focal segmental glomerulosclerosis. *J Am Soc Nephrol* 2000; **11**: 403–412.
7. Raats CJ, van Den Born J, Bakker MA *et al.* Expression of agrin, dystroglycan, and utrophin in normal renal tissue and in experimental glomerulopathies. *Am J Pathol* 2000; **156**: 1749–1765.

8. Williamson RA, Henry MD, Daniels KJ *et al.* Dystroglycan is essential for early embryonic development: disruption of Reichert's membrane in *Dag1*-null mice. *Hum Mol Genet* 1997; **6**: 831–841.
9. Fukuyama Y, Osawa M, Suzuki H. Congenital progressive muscular dystrophy of the Fukuyama type-clinical, genetic, and pathological considerations. *Brain Dev* 1981; **3**: 1–29.
10. Toda T, Segawa M, Nomura Y *et al.* Localization of a gene for Fukuyama type congenital muscular dystrophy to chromosome 9q31-33. *Nat Genet* 1993; **5**: 283–286.
11. Toda T, Miyake M, Kobayashi K *et al.* Linkage-disequilibrium mapping narrows the Fukuyama-type congenital muscular dystrophy (FCMD) candidate region to <100 kb. *Am J Hum Genet* 1996; **59**: 1313–1320.
12. Takeda S, Kondo M, Sasaki J *et al.* Fukutin is required for maintenance of muscle integrity, cortical histiogenesis and normal eye development. *Hum Mol Genet* 2003; **12**: 1449–1459.
13. Ruotsalainen V, Ljungberg P, Wartiovaara J *et al.* Nephrin is specifically located at the slit diaphragm of glomerular podocytes. *Proc Natl Acad Sci USA* 1999; **96**: 7962–7967.
14. Hemler ME. Dystroglycan versatility. *Cell* 1999; **97**: 543–546.
15. Durbeej M, Henry MD, Campbell KP. Dystroglycan in development and disease. *Curr Opin Cell Biol* 1998; **10**: 594–601.
16. Hohenester E, Tisi D, Talts JF *et al.* The crystal structure of a laminin G-like module reveals the molecular basis of alpha-dystroglycan binding to laminins, perlecan, and agrin. *Mol Cell* 1999; **4**: 783–792.
17. Kojima K, Davidovits A, Poczewski H *et al.* Podocyte flattening and disorder of glomerular basement membrane are associated with splitting of dystroglycan-matrix interaction. *J Am Soc Nephrol* 2004; **15**: 2079–2089.
18. Vogtländer NPJ, Tamboer WPM, Bakker MAH *et al.* Reactive oxygen species deglycosilate glomerular α-dystroglycan. *Kidney Int* 2006; **69**: 1526–1534.
19. Kitsiou PV, Tzinia AK, Stetler-Sterenson WG *et al.* Glucose-induced changes in integrins and matrix-related function in cultured human glomerular epithelial cells. *Am J Physiol* 2003; **285**: F40–F48.
20. Kreidberg JA, Donovan MJ, Goldstein SL *et al.* Alpha 3 beta 1 integrin has a crucial role in kidney and lung organogenesis. *Development* 1996; **122**: 3537–3547.
21. Andrews PM. Glomerular epithelial alterations resulting from sialic acid surface coat removal. *Kidney Int* 1979; **15**: 376–385.
22. Galeano B, Klootwijk R, Manoli I *et al.* Mutation in the key enzyme of sialic acid biosynthesis causes severe glomerular proteinuria and is rescued by *N*-acetylmannosamine. *J Clin Invest* 2007; **117**: 1585–1594.
23. Chen S, Wassenhove-McCarthy DJ, Yamaguchi Y *et al.* Loss of heparan sulfate glycosaminoglycan assembly in podocytes does not lead proteinuria. *Kidney Int* 2008; **74**: 289–299.
24. Kestila M, Ienkkeri U, Mannikko M *et al.* Positionally cloned gene for a novel glomerular protein—nephrin—is mutated in congenital nephrotic syndrome. *Mol Cell* 1998; **1**: 575–582.
25. Tryggvason K, Ruotsalainen V, Wartiovaara J. Discovery of the congenital nephrotic syndrome gene discloses the structure of the mysterious molecular sieve of the kidney. *Int J Dev Biol* 1999; **43**: 445–451.
26. Doublier S, Routsalainen V, Salvidio G *et al.* Nephrin redistribution on podocytes is a potential mechanism for proteinuria in patients with primary acquired nephrotic syndrome. *Am J Pathol* 2001; **158**: 1723–1731.
27. Wernerson A, Duner F, Pettersson E *et al.* Altered ultrastructural distribution of nephrin in minimal change nephrotic syndrome. *Nephrol Dial Transplant* 2003; **18**: 70–76.
28. Kurahashi H, Taniguchi M, Meno C *et al.* Basement membrane fragility underlies embryonic lethality in *fukutin*-null mice. *Neurobiol Dis* 2005; **19**: 208–217.
29. Colognato H, Winkelmann DA, Yurchenco PD. Laminin polymerization induces a receptor-cytoskeleton network. *J Cell Biol* 1999; **145**: 619–631.
30. Saito F, Masaki T, Saito Y *et al.* Defective peripheral nerve myelination and neuromuscular junction formation in fukutin-deficient chimeric mice. *J Neurochem* 2007; **101**: 1712–1722.
31. Kawachi H, Koike H, Kurihara H *et al.* Cloning of rat nephrin: expression in developing glomeruli and in proteinuric states. *Kidney Int* 2000; **57**: 1949–1961.

Fukutin and Fukuyama Congenital Muscular Dystrophy

Motoi Kanagawa[1], Tatsushi Toda[2]

Introduction

Recent genetic and biochemical studies have revealed that mutations in (putative) glycosyltransferases and subsequent abnormal glycosylation of dystroglycan are associated with several forms of congenital muscular dystrophies (Kanagawa and Toda 2006). Fukuyama congenital muscular dystrophy (FCMD), the second most common childhood muscular dystrophy in Japan, is one of the congenital muscular dystrophies displaying glycosylation defects of α-dystroglycan. The gene responsible for this disease is *fukutin*, and its protein product is assumed to participate in cellular glycosylation events. FCMD is characterized by severe congenital muscular dystrophy, abnormal neuronal migration associated with mental retardation and epilepsy, and frequent eye abnormalities. Therefore, fukutin-dependent glycosylation of α-dystroglycan plays crucial roles in structural/functional maintenance of skeletal muscle, central/peripheral nervous system, and eye. α-Dystroglycan, a highly glycosylated protein, forms a protein complex with β-dystroglycan, and the dystroglycan complex links laminin in the extracellular matrix to the cellular actin cytoskeleton. Abnormal glycosylation of α-dystroglycan results in a severe reduction in laminin-binding activity, and thus disruption of the interaction between dystroglycan and laminin caused by *fukutin* mutations is believed to be the major cause of FCMD.

Fukutin

The gene responsible for FCMD was identified by positional cloning and its protein product was named as fukutin (Kobayashi et al. 1998). The major mutation in FCMD is a 3-kb retrotransposon insertion in the 3′ noncoding region of the *fukutin* gene. Some FCMD patients carrying point-mutation(s) in the *fukutin* gene have also been reported. The function of fukutin is still unknown; however, computer analysis has predicted that fukutin has homology to enzymes that modify glycolipids and glycoproteins. Fukutin, a 461-amino-acid protein with a predicted molecular weight of 53.7 kDa, is a type-II membrane protein and possesses a DXD motif. Fukutin has been shown to localize to the Golgi apparatus. In FCMD muscle, α-dystroglycan is hypoglycosylated and its ligand-binding activities are dramatically decreased. These findings indicate that fukutin is involved in the glycosylation pathway of α-dystroglycan. A recent study has demonstrated the possibility that fukutin interacts with and regulates POMGnT1, which synthesizes *O*-mannosylglycan on α-dystroglycan (for details on POMGnT1 see Chapter by

[1,2]Division of Clinical Genetics, Department of Medical Genetics, Osaka University Graduate School of Medicine, 2-2-B9 Yamadaoka, Suita, Osaka 565-0871, Japan
Phone: +81-6-6879-3381, Fax: +81-6-6879-3389
E-mail: [1]kanagawa@clgene.med.osaka-u.ac.jp, [2]toda@clgene.med.osaka-u.ac.jp

T. Endo and H. Manya and Chapter by T. Endo, in this volume). Generation of fukutin chimeric mice confirmed the essential role of fukutin-dependent glycosylation of dystroglycan in the maintenance of muscle integrity, cortical histiogenesis, and ocular development. Targeted homozygous mutation of the *fukutin* gene in mice leads to embryonic lethality prior to the development of skeletal muscle and mature neurons. Detailed analyses of *fukutin*-null embryos suggested that fukutin is necessary for the maintenance of basement membrane function during early embryonic development.

Abnormal Glycosylation of Dystroglycan in FCMD

α/β-Dystroglycan is encoded by a single mRNA and is post-translationally cleaved into two subunits. α-Dystroglycan is a receptor for laminin, a major component of the extracellular matrix, and *O*-glycosylation of α-dystroglycan is essential for its laminin-binding activity. α-Dystroglycan is anchored on the plasma membrane through the non-covalent interaction with β-dystroglycan. β-Dystroglycan is a transmembrane protein and interacts intracellularly with dystrophin. Therefore, the dystroglycan complex acts as a linkage between the extracellular matrix and the dystrophin-actin cytoskeleton across the muscle plasma membrane (Kanagawa and Toda 2006). This interaction is believed to provide mechanical integrity to the muscle cell membrane. Since fukutin defects result in aberrant glycosylation of dystroglycan with reduced ligand-binding activity, the dystroglycan-mediated linkage between the extracellular matrix and the cytoskeleton is likely to be disrupted in FCMD, which renders the muscle cell membrane to be fragile and more susceptible to mechanical stress by muscle contraction, eventually leading to muscle cell wasting.

Abnormal glycosylation of α-dystroglycan can be tested by immunofluorescence or Western blotting analysis using monoclonal antibodies that recognize the functionally glycosylated form of α-dystroglycan (IIH6 and VIA4–1) and polyclonal antibodies that recognize the α-dystroglycan core peptide (GT20ADG). Abnormally glycosylated α-dystroglycan loses reactivity against IIH6 and VIA4–1, and shows a reduced molecular weight that can be detected by Western blotting with the α-dystroglycan core antibodies (Michele et al. 2002). A monoclonal antibody to β-dystroglycan (8D5) can be used to confirm the amount of dystroglycan protein expressed.

Glycotherapy for FCMD

Since defects in laminin-binding glycans on α-dystroglycan are a cause of FCMD, therefore complementing glycans, having affinity to laminin, on α-dystroglycan could be a therapeutic strategy of FCMD. LARGE, a putative glycosyltransferase involved in the functional glycosylation of dystroglycan, is a potential target for glycotherapy. Overexpression of LARGE produces hyperglycosylated α-dystroglycan with increased ligand-binding activity in cells from FCMD patients (Barresi et al. 2004). Although the detailed mechanism of LARGE-dependent hyperglycosylation of α-dystroglycan is still unclear, this finding may lead to a novel strategy to treat FCMD and related congenital muscular dystrophies by bypassing the alternative dystroglycan-laminin linkage. Thus, glycotherapies and treatments aimed at modulating the expression or the activity of LARGE may be a future therapeutic option for glycosyltransferase-deficient muscular dystrophies.

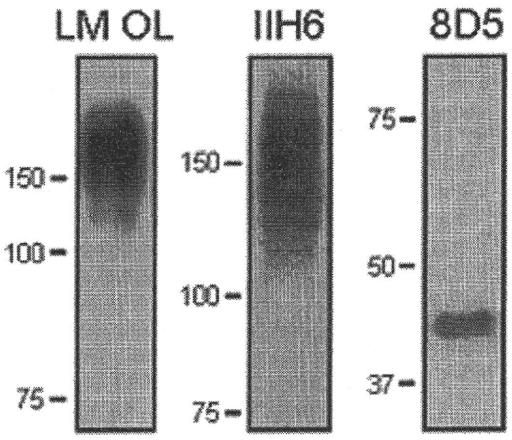

Fig. 1 Laminin overlay assay and Western blotting analysis of dystroglycan. WGA-purified preparations from mouse skeletal muscle extracts were analyzed by laminin overlay assay (LM OL) and Western blotting. IIH6 and 8D5 are monoclonal antibodies to α-dystroglycan and β-dystroglycan, respectively

Laminin Overlay Assay

Laminin-binding activity of α-dystroglycan can be determined by the laminin overlay assay (Fig. 1) and the solid-phase laminin-binding assay (Michele et al. 2002). In this chapter, the protocol of the laminin overlay assay is described (for the solid-phase laminin-binding assay, see Michele et al. 2002).

Laminin-binding buffer (LBB): 10 mM triethanolamine-HCl (pH 7.4), 140 mM NaCl, 1 mM $CaCl_2$, 1 mM $MgCl_2$

1. Subject tissue/cell extracts or dystroglycan preparations to SDS-PAGE (dystroglycan can be enriched by WGA- or Con A-affinity chromatography).
2. Transfer separated proteins to a PVDF membrane and block the blot with 5% skim milk/LBB at room temperature.
3. Briefly wash the blot with 3% BSA/LBB.
4. Incubate the blot with 1–10 nM laminin in 3% BSA/LBB at 4°C for >12 h.
5. After washing with 5% skim milk/LBB, incubate the blot with an anti-laminin antibody at room temperature for several hours.
6. After washing with 5% skim milk/LBB, incubate the blot with the appropriate HRP-conjugated secondary antibody at room temperature for 1 h.
7. After washing with LBB, develop the blot by enhanced chemiluminescence.

Comment

Laminin-binding activity of dystroglycan varies in different tissues and cell types. Skeletal muscle dystroglycan can be used as a positive control (~150 kDa).

Acknowledgments The work from our laboratory was supported by the 21st Century COE program (Integrated functional analyses of disease-associated sugar chains and proteins) from the Ministry of Education, Culture, Sports, Science, and Technology of Japan.

References

Barresi R, Michele DE, Kanagawa M, Harper HA, Dovico SA, Satz JS, Moore SA, Zhang W, Schachter H, Dumanski JP, Cohn RD, Nishino I, Campbell KP (2004) LARGE can functionally bypass alpha-dystroglycan glycosylation defects in distinct congenital muscular dystrophies. Nat Med 10:696–703

Kanagawa M, Toda T (2006) The genetic and molecular basis of muscular dystrophy: roles of cell-matrix linkage in the pathogenesis. J Hum Genet 51:915–926

Kobayashi K, Nakahori Y, Miyake M, Matsumura K, Kondo-Iida E, Nomura Y, Segawa M, Yoshioka M, Saito K, Osawa M, Hamano K, Sakakihara Y, Nonaka I, Nakagome Y, Kanazawa I, Nakamura Y, Tokunaga K, Toda T (1998) An ancient retrotransposal insertion causes Fukuyama-type congenital muscular dystrophy. Nature 394:388–392

Michele DE, Barresi R, Kanagawa M, Saito F, Cohn RD, Satz JS, Dollar J, Nishino I, Kelley RI, Somer H, Straub V, Mathews KD, Moore SA, Campbell KP (2002) Post-translational disruption of dystroglycan-ligand interactions in congenital muscular dystrophies. Nature 418:417–422

J. Biochem. 2010;147(3):337–344 doi:10.1093/jb/mvp170

JB THE JOURNAL OF BIOCHEMISTRY

Role of *N*-glycans in maintaining the activity of protein *O*-mannosyltransferases POMT1 and POMT2

Received September 18, 2009; accepted October 13, 2009; published online October 29, 2009

Hiroshi Manya[1,*], Keiko Akasaka-Manya[1], Ai Nakajima[1,2], Masao Kawakita[2] and Tamao Endo[1]

[1]Glycobiology Research Group, Tokyo Metropolitan Institute of Gerontology, Foundation for Research on Aging and Promotion of Human Welfare, 35-2 Sakaecho, Itabashi-ku, Tokyo 173-0015; and [2]Department of Applied Chemistry, Kogakuin University, Tokyo 163-8677, Japan

*Hiroshi Manya. Glycobiology Research Group, Tokyo Metropolitan Institute of Gerontology, Foundation for Research on Aging and Promotion of Human Welfare, 35-2 Sakaecho, Itabashi-ku, Tokyo 173-0015, Japan, Tel: 81-3-3964-3241, Ext. 3055, Fax: 81-3-3579-4776, E-mail: manya@tmig.or.jp.

The complex of protein *O*-mannosyltransferase 1 (POMT1) and POMT2 catalyzes the initial step of *O*-mannosyl glycan biosynthesis. The mutations in either *POMT1* or *POMT2* can lead to Walker–Warburg syndrome, a congenital muscular dystrophy with abnormal neuronal migration. Here, we used three algorithms for predicting transmembrane helices to construct the secondary structural models of human POMT1 and POMT2. In these models, POMT1 and POMT2 have seven- and nine-transmembrane helices and contain four and five potential *N*-glycosylation sites, respectively. To determine whether these sites are actually glycosylated, we prepared mutant proteins that were defective in each site by site-directed mutagenesis. Three of the POMT1 sites and all of the POMT2 sites were found to be *N*-glycosylated, suggesting that these sites face the luminal side of the endoplasmic reticulum. Mutation of any single site did not significantly affect POMT activity, but mutations of all *N*-glycosylation sites of either POMT1 or POMT2 caused a loss of POMT activity. The loss of activity appeared to be due to the decreased hydrophilicity. These results suggest that the *N*-glycosylation of POMT1 and POMT2 is required for maintaining the conformation as well as the activity of the POMT1-POMT2 complex.

Keywords: *N*-glycosylation/protein *O*-mannosyltransferase/POMT1/POMT2/secondary structure.

Abbreviations: α-DG, α-Dystroglycan; Dol-P-Man, dolichyl phosphate mannose; ER, endoplasmic reticulum; Man, mannose; SDS–PAGE, sodium dodecyl sulfate-polyacrylamide gel electrophoresis; WWS, Walker–Warburg syndrome; POMT1, protein *O*-mannosyltransferase 1; POMT2, protein *O*-mannosyltransferase 2; HEK, Human embryonic kidney.

Protein *O*-mannosyltransferase 1 (POMT1) and POMT2 (POMT, EC 2.4.1.109), which are located in the endoplasmic reticulum (ER) membrane, catalyze the initial step of *O*-mannosyl glycans biosynthesis, *i.e.* the transfer of a mannosyl residue from dolichyl phosphate mannose (Man) (Dol-P-Man) to Ser/Thr residues of certain proteins (*1*). Mutations in *POMT1* and *POMT2* are reported to cause Walker–Warburg syndrome (WWS: OMIM 236670), an autosomal recessive developmental disorder associated with congenital muscular dystrophy, neuronal migration defects and ocular abnormalities (*2*, *3*). Previously, we found that α-dystroglycan (α-DG) was predominantly modified by *O*-mannosyl glycans, Siaα2-3Galβ1-4GlcNAcβ1-2Man (*4*), and reported that defects in *O*-mannosyl glycan on α-DG cause several α-dystroglycanopathies, which are a group of congenital muscular dystrophies that include WWS, muscle–eye–brain disease (MEB: OMIM 253280) and Fukuyama congenital muscular dystrophy (FCMD: OMIM 253800) (*5*, *6*). α-DG is a component of the dystrophin–glycoprotein complex that acts as a transmembrane linker between the extracellular matrix and intracellular cytoskeleton (*7*). *O*-Mannosyl glycans of α-DG have a role in binding to extracellular matrixes such as laminin, neurexin and agrin (*4*, *8–11*). When α-DG fails to bind to laminin or other molecules in the extracellular matrix as a result of a defect in α-DG glycosylation, it is thought to interrupt normal muscular function and migration of neurons in the developing brain (*12*). Thus, *O*-mannosyl glycans are indispensable for normal structure and function of α-DG in muscle and brain.

Several mutations in the *POMT1* and *POMT2* genes were identified in patients with WWS (*2*, *3*, *13*). We previously demonstrated that these mutations lead to defects of POMT activity (*13*, *14*). We also confirmed that formation of a complex of POMT1 and POMT2 was required for POMT activity (*15*). However, the mechanism(s) by which the mutations cause a loss of POMT activity and the significance of complex formation remain unclear. POMT1 and POMT2 are homologous to protein *O*-mannosyltransferases (PMTs) in yeast. *Saccharomyces cerevisiae* has seven pmts (pmt1–7) that form hetero and homo complexes in various combinations (*16*). Yeast pmt1 has been proposed to consist of seven transmembrane helices (*17*). The pmt1 N-terminus and loops 2, 4 and 6 are located in the cytoplasm, and the C-terminus and loops 1, 3 and 5 are located in the ER lumen. A large hydrophilic region (loop 5) and loop 1 have been reported to be important for enzymatic activity (*17–19*).

Glycoprotein glycans strongly affect various biological and physical properties of proteins, such as their stabilities, conformations, interactions, cellular localizations and trafficking. The presence or absence of *N*-glycans in PMTs, as well as their structures and roles has not yet been ascertained. Human POMT1 and POMT2 contain four and five potential *N*-glycosylation sites, respectively. In the present study, we used three algorithms for predicting transmembrane helices to construct models of the secondary structures of human POMT1 and POMT2, and determined the topology of both POMTs by analyzing the *N*-glycosylation status of potential site. Furthermore, by removing potential *N*-glycosylation sites, we showed that the *N*-glycans are required for POMT activity.

Materials and methods

Vector construction of POMT1 and POMT2 mutants

cDNAs for the most common splicing variant of human myc-tagged *POMT1* (lacking bases 700–765, corresponding to amino acids 234–255) and non-tagged *POMT2* were used for site-directed mutagenesis and cloned into pcDNA 3.1 (Invitrogen Corp., Carlsbad, CA, USA), as described previously (*15*). The *POMT1* and *POMT2* genes were modified with a QuickChange Site-Directed Mutagenesis Kit (STRATAGENE, La Jolla, CA, USA) according to the manufacturer's instructions. All mutant clones were sequenced to confirm the presence of the mutations. The primer pairs used to make the mutants were: N16Q, 5′-GTGACGGCTGACATCCAATTGAGCCTTGTGGCC-3′ and 5′-GGCCACAAGGCTCAATTGGATGTCAGCCGTCAC-3′; N435Q, 5′-CCTGCTACATTGACTATCAAATCTCCATGCCCGCCC-3′ and 5′-CCTGCTACATTGACTATCAAATCTCCATGCCCGCCC-3′; N471Q, 5′-GTCCGCTTTGTGCACGTGCAAACTTCCGCTGTC-3′ and 5′-GACAGCGGAAGTTTGCACGTGCACAAAGCGGAC-3′; N539Q, 5′-GGTGGACGTCAGCAGGCAACTCAGCTTCATGG-3′ and 5′-CCATGAAGCTGAGTTGCCTGCTGACGTCCACC-3′; N98Q, 5′-GTTACTATATCCAACGTACATTTTTCTTTGATGTGCACCCGCC-3′ and 5′-GGCGGGTGCACATCAAAGAAAAATGTACGTTGGATATAGTAAC-3′; N330Q, 5′-CAGGGAACAACCTGCACCAAGCTTCCATCCCTG-3′ and 5′-CAGGGATGGAAGCTTGGTGCAGGTTGTTCCCTG-3′; N445Q, 5′-GGTCACCGGATATGGCATACAAGGAACAGGGGAC-3′ and 5′-GTCCCCTGTTCCTTGTATGCCATATCCGGTGACC-3′; N528Q, 5′-CCCAAGTTGCCACAAATCAGCCTGGATGTGCTACAG-3′ and 5′-CTGTAGCACATCCAGGCTGATTTGTGGCAACTTGGG-3′; N583Q, 5′-CGCTTCTCAGGGGTCCAAGACACAGATTTCCGAG-3′ and 5′-CTCGGAAATCTGTGTCTTGGACCCCTGAGAAGCG-3′.

Expression of POMTs and preparation of microsomal fraction

Human embryonic kidney (HEK) 293T cells were maintained in Dulbecco's modified Eagle's medium (Invitrogen) supplemented with 10% fetal bovine serum, 2 mM L-glutamine, 100 units/ml penicillin and 50 μg/ml streptomycin at 37°C with 5% CO_2. Expression plasmids were transfected into HEK293T cells using Lipofectamine Plus reagent (Invitrogen) according to the manufacturer's instructions. Cells were incubated for 3 days to produce POMT1 and POMT2 proteins. The cells were homogenized in 10 mM Tris–HCl, pH 7.4, 1 mM EDTA, 250 mM sucrose, 1 mM DTT, with protease inhibitor mixture (3 μg/ml pepstatin A, 1 μg/ml leupeptin, 1 mM benzamidine-HCl, 1 mM PMSF). After centrifugation at 900*g* for 10 min, the supernatant was subjected to ultracentrifugation at 100,000*g* for 1 h. The precipitate was used as the microsomal fraction. Protein concentration was determined by BCA assay (Thermo Fisher Scientific Inc., Waltham, MA, USA). Microsomal fractions were solubilized with 20 mM Tris–HCl, pH 8.0, 2 mM 2-mercaptoethanol, 10 mM EDTA and 0.5% *n*-octyl-β-D-thioglucoside at 4°C. After centrifugation at 10,000*g* for 10 min, the supernatant was used as solubilized supernatant.

To examine the effects of tunicamycin, tunicamycin was added to the culture medium after transfection at a final concentration of 1 μg/ml, and the culture was continued for 3 days. A microsomal fraction and a solubilized microsomal fraction were obtained as described earlier.

Western blot analysis

The microsomal fractions (20 μg) or solubilized supernatants were separated by sodium dodecyl sulfate-polyacrylamide gel electrophoresis (SDS–PAGE) (7.5% gel) and proteins were transferred to a polyvinylidene difluoride membrane. The membrane was blocked in PBS containing 5% skim milk and 0.05% Tween 20, incubated with anti-myc (A-14) antibody (Santa Cruz Biotech, Santa Cruz, CA, USA) or anti-POMT2 polyclonal antibody (*15*), and treated with anti-goat IgG conjugated with HRP (Santa Cruz Biotech) or anti-rabbit IgG conjugated with horseradish peroxidase (HRP) (GE Healthcare Bio-sciences Corp., Piscataway, NJ, USA). Proteins that bound to the antibody were visualized with an ECL kit (GE Healthcare Bio-sciences). As reported previously (*15*), anti-POMT2 antibody did not detect endogenous POMT2 but was specific to recombinant POMT2.

Assay for POMT activity

POMT activity was based on the amount of [^{3}H]-mannose transferred to a glutathione-S-transferase fusion α-dystroglycan (GST-α-DG) as described previously (*1*). The reaction mixture contained 20 mM Tris–HCl (pH 8.0), 100 nM of [^{3}H]-mannosylphosphoryldolichol (Dol-P-Man, 125,000 dpm/pmol) (American Radiolabeled Chemical, Inc., St Louis, MO, USA), 2 mM 2-mercaptoethanol, 10 mM EDTA, 0.5% *n*-octyl-β-D-thioglucoside, 10 μg GST-α-DG and enzyme source (80 μg of microsomal membrane fraction) in 20 μl total volume. After 1 h incubation at 22°C, the reaction was stopped by adding 150 μl PBS containing 1% Triton X-100 (Nacalai Tesque, Kyoto, Japan), and the reaction mixture was centrifuged at 10,000g for 10 min. The supernatant was removed, mixed with 400 μl of PBS containing 1% Triton X-100 and 10 μl of Glutathione-Sepharose 4B beads (GE Healthcare Bio-sciences), rotated at 4°C for 1 h, and washed three times with 20 mM Tris–HCl (pH 7.4) containing 0.5% Triton X-100. The radioactivity adsorbed to the beads was measured using a liquid scintillation counter.

Endo-glycosidase digestion

N-glycosidase F (PNGase F) and endoglycosidase H (Endo H) were purchased from Roche Diagnostics K.K. (Basel, Switzerland). The microsomal fraction (100 μg) was denatured with boiling for 3 min in denaturation buffer (40 μl) containing 0.1 M citrate-phosphate buffer containing 0.1% SDS, 20 mM EDTA and 10 mM 2-mercaptoethanol. After the mixture was cooled, 40 μl dilution buffer containing 0.1 M citrate-phosphate buffer and 2 U of PNGase F or 0.01 U of Endo H were added. The mixture was incubated at 37°C for 6 h. The pH values of the citrate-phosphate buffers were 7.0 for PNGase F or 5.5 for Endo H.

Results

Transmembrane prediction of human POMT1 and POMT2

The yeast *O*-mannosyltransferase pmt1 is proposed to have seven-transmembrane helices (*17*). In this study, the transmembrane topologies of human POMT1 and POMT2 were predicted with three algorithms specifically designed to detect transmembrane alpha helices: SOSUI (*20*), TMPred (*21*) and HMMTOP (*22*). The helices predicted by the three algorithms are shown by the colored underlines in Fig. 1, and as the consensus helices are highlighted in yellow. These results suggest that POMT1 and POMT2 have seven and nine transmembrane helices, respectively.